

Synchronization of Globally Coupled Nonlinear Oscillators:  
the Rich Behavior of the Kuramoto Model

Bryan C. Daniels

May 6, 2005

### **Abstract**

Global synchronization of oscillators is found abundantly in nature, emerging in fields from physics to biology. The Kuramoto model describes the synchronization behavior of a generalized system of interacting oscillators. With a large number of oscillators with different natural frequencies, the Kuramoto model predicts that, if they are allowed to interact strongly enough, they will all start oscillating at the same rate. The model provides a mathematical basis for studying the conditions under which synchronization can occur. For example, it is possible to solve for the critical amount of coupling needed among the oscillators to have synchronization. My research involved studying the basics of Kuramoto's analysis and then investigating how the synchronization behavior is affected by random noise. Numerical simulations were run with and without noise to supplement and verify the analytical results.

# Contents

<b>1</b>	<b>Introduction to Synchronization</b>	<b>3</b>
1.1	Historical Overview . . . . .	3
1.2	Defining Synchronization . . . . .	4
1.3	Where We Find Mutual Synchronization . . . . .	5
1.4	Mathematical Background . . . . .	6
1.5	The Kuramoto Model . . . . .	7
<b>2</b>	<b>Kuramoto's Model of Coupled, Nonlinear Oscillators</b>	<b>11</b>
2.1	Solving for $K_C$ . . . . .	11
2.1.1	Mean-Field Parameters . . . . .	11
2.1.2	Steady Solutions . . . . .	12
2.1.3	Solving for the Order Parameter and $K_C$ . . . . .	14
2.2	The Growing Order Parameter . . . . .	15
2.2.1	Initial Growth . . . . .	15
2.2.2	Lorentzian density . . . . .	17
2.3	Numerical Simulations . . . . .	18
<b>3</b>	<b>Adding Noise to the Kuramoto Model</b>	<b>21</b>
3.1	An Example of a Stochastic Process . . . . .	21
3.2	The Continuum Limit <sup>1</sup> . . . . .	23
3.3	Adding Noise to the Kuramoto Model . . . . .	25
3.3.1	The Fokker-Planck Equation . . . . .	26
<b>4</b>	<b>The Effects of Noise: Stability Analysis</b>	<b>27</b>
4.1	Adding a Perturbation . . . . .	28

4.2	Fourier Methods . . . . .	30
4.3	Evolution of the Fundamental Mode . . . . .	31
4.3.1	Finding the Separable Solutions . . . . .	31
4.3.2	Finding $K_C$ with Noise . . . . .	33
4.3.3	Solving Explicitly for the Eigenvalue . . . . .	33
4.3.4	The Continuous Spectrum . . . . .	34
4.4	Numerical Simulations with Noise . . . . .	36
4.5	Evolution of Higher Harmonics . . . . .	37
4.6	Second Order Stability Analysis . . . . .	38
4.6.1	Adding the Second Order Perturbation . . . . .	38
4.6.2	Fourier Methods . . . . .	40
	<b>Conclusion</b>	<b>42</b>
	<b>Acknowledgments</b>	<b>43</b>
	<b>A The Vanishing Drift Integral</b>	<b>44</b>
	<b>B Deriving a Fokker-Planck Equation for the Kuramoto Model</b>	<b>46</b>
	<b>C Example FORTRAN Code</b>	<b>48</b>
	<b>References</b>	<b>54</b>

# Chapter 1

## Introduction to Synchronization

### 1.1 Historical Overview

The story of synchronization begins with an ill Dutch scientist. In 1665, Christiaan Huygens was lying in bed, sick, with the ticking of the clock keeping him company. In fact, there were two pendulum clocks hanging on the wall in his room; in earlier years, he had worked hard to invent and perfect the design of these timepieces. During a few days spent watching the clocks, he made an observation that he found interesting enough to include in his next letter to his father. He noticed that the pendula always moved so that when one was furthest left, the other was furthest right, and vice versa, so that they always moved opposite of one another. Huygens was intrigued and tested the phenomenon by disturbing the rhythm—and the clocks always came back to the same relative orientation. Of course, being a scientist, he looked for an explanation for what he called the “sympathy of two clocks.” He decided that each pendulum caused an imperceptible motion in the beam of the wall from which they were hanging, and that this motion tended to force the other pendulum toward moving in synchrony with it. Once the pendula were synchronized like this, their opposite forces would cancel and the beam would stay still [1, 1-3].

It turns out that Huygens was right; besides some differences in the terminology, this is exactly the explanation we have today for the phenomenon of mutual synchronization. Modern scientists would call the motion of the beam the coupling between the clocks, and the type of synchronization anti-phase (since the pendula are moving opposite of one another). These are general terms used to describe many different types of systems; as we will see, what makes the study of synchronization so interesting today is that it is far from limited to pendulum clocks [1, 7-14].

In the 1920s, for example, triode generators were coupled and were found to synchronize. A triode gener-

ator produces an alternating electrical current, and the frequency of this oscillation depends on parameters of the elements that make up the generator. Two different generators will in general produce different frequencies of alternating current; but when the two generators are coupled, they synchronize to produce the same frequency. Furthermore, theoretical studies showed that the generators could be entrained even by a weak external signal. This result was used to create powerful generators that could be tuned to a very specific frequency by synchronizing them to a much weaker but more precise generator [1, 4-5].

Biologists were also noticing synchronization in organisms. Jean-Jacques Dortous de Mairan discovered in 1729 that haricot bean plants have leaves that move up and down with the daily cycle of darkness and light. In addition, he found that the leaves still move at a nearly 24-hour cycle in a dark room, without the influence of sunlight. Extensive studies since that time have proven the existence of internal biological clocks that regulate the circadian (daily) rhythms of organisms. In the absence of outside influences (the light of the sun, for example), these clocks may differ slightly from a 24-hour cycle, but in normal conditions they are synchronized to the day-night cycle by external cues [1, 5-7].

With these and other examples it became clear that synchronization was some kind of ubiquitous phenomenon in nature, so scientists set out to more deeply understand the principles behind it. Even today, the study of synchronization is far from complete, making it an exciting topic for research. The remainder of this chapter will introduce the basic concepts in the study of synchronization along with an introduction of the more specific area of the field that I will focus on in my research.

## 1.2 Defining Synchronization

Before we can get into the in-depth study of synchronization, we need a more thorough description of what we mean by the term. One definition of synchronization found in the literature is an “adjustment of rhythms of oscillating objects due to their weak interaction” [1, 8]. We can further describe “oscillating objects” as systems that are driven into oscillation by an energy source and are stable in their oscillations to small perturbations. So when we study synchronization, we are generally looking at objects that would oscillate alone, without outside influence. These are called self-sustaining oscillators. With more than one of these oscillating objects, interactions can occur. These interactions are called coupling, and the coupling strength describes how strong the interactions are. Even with weak coupling (as Huygens saw with his clocks), non-identical oscillators can interact in such a way to synchronize to each other. Generally, a group of oscillators is said to be synchronized when each oscillator’s frequency has locked onto the same value as all the others’ [1, 8-10].

There are generally two values that determine how easily a group of oscillators can synchronize: the

coupling strength, described above, and the frequency detuning. Frequency detuning is a number describing how different the natural frequencies of the oscillators are in the absence of the effects of the other oscillators. In theoretical studies, the natural frequencies are generally described by some distribution function<sup>1</sup>, so the frequency detuning would be some measure of the width of this distribution. A group with large frequency detuning is harder to synchronize because the individual oscillators want to oscillate at highly varied frequencies. All interacting oscillators have a range of values for the detuning for which they are able to synchronize. Inside this range, the coupling causes the oscillators to have the exact same frequency (not just close, as one would expect even without coupling); this range typically expands as the coupling strength increases [1, 11-12].

Once frequency synchronization has occurred, we can also look at relationships that form between the phases of the interacting oscillators. In the case of Huygens' two interacting clocks, the oscillators synchronized in anti-phase—one pendulum was furthest to the left when the other was furthest to the right. We can also observe in-phase synchronization, when the oscillators are locked exactly to each other, each one always at the same point in the cycle as the others [1, 14].

### 1.3 Where We Find Mutual Synchronization

As mentioned before, synchronization is observed abundantly in nature. A particularly beautiful example comes from certain species of fireflies that have captured the attention of many Western travelers in southeast Asia for hundreds of years. The travelers come back with stories of huge populations of fireflies all flashing in perfect unison, making long swaths of light flashing on and off in the darkness. It was not until the late 1960s that anyone understood what was really going on—that the rhythm was not being set by any single “conductor” firefly, but rather by the interactions among all of them. Somehow the oscillator in each firefly (presumably some patch of neurons in each firefly's brain) corrects itself to flash in unison with all the others [2]. Unlike the generator and circadian rhythm examples, which concern a single oscillator synchronizing to an external stimulus, here we have a large population of non-identical oscillators that all synchronize to the same frequency and phase by their mutual interactions alone.

In fact, the type of mutual synchronization exemplified by the fireflies is very prevalent in nature. A similar example comes from audiences in Eastern Europe, where it is common for applause to become synchronized across large groups of audience members [1, 131]. Synchronization of menstrual cycles of women in close contact with one another has also been studied [1, 129]. Muscle contractions are another important example. Mammalian intestinal muscles, for example, have been found to synchronize to neighboring muscles to have

---

<sup>1</sup>A Gaussian distribution is one possibility, for example. See Figure 2.2 on page 17 for a plot of some sample distributions.

the same rate of contraction [1, 121]. Heart muscles exhibit the same kind of behavior, synchronizing to each other to create a coherent heartbeat [1, 112].

Aside from these biological examples, there are manmade systems that exhibit the same kind of behavior. Specifically, Josephson junctions are fabricated, microscopic devices that behave as compact electronic oscillators and emit microwaves under controlled conditions. Different geometric arrangements of Josephson junctions form systems of oscillators that have been found theoretically to exhibit synchronization and to be amenable to analytical studies and computer simulation [1, 291-4].

## 1.4 Mathematical Background

The study of synchronization involves many mathematical abstractions; the most fundamental of these is the idea of a phase space. The phase space of a system is formed by variables that describe the state of the system. For example, the state of a pendulum could be described by its position (specified by an angle) and its velocity, giving it a two-dimensional phase space. This means the state of the system at a given time is shown as a certain point in the phase space. As the system evolves, the point moves in some trajectory in the phase space. To describe the motion of an oscillator, then, we can talk about its motion in phase space. Self-sustained oscillators like the ones studied in this paper move in phase space in a special way—when left to themselves, they eventually revisit the same points over and over. So the steady-state evolution of a self-sustained oscillator corresponds to some closed curve in phase space [1, 29].

This closed curve is called a limit cycle. Self-sustained oscillations have stable limit cycles, meaning that all trajectories near the limit cycle approach the limit cycle. This is the same as saying that the oscillator is stable to perturbations—after taking it slightly away from its limit cycle, it will eventually come back to oscillate in the original cycle [1, 29-30][3, 196]. Figure 1.1 shows a sample limit cycle for a self-sustained oscillator.

To determine the phase relationship among different oscillators (to find if they are in-phase or in anti-phase, for example), we must define the phase of the system. For self-sustained oscillators the phase  $\phi$  is defined so that it grows uniformly in time and gains  $2\pi$  radians for each trip around the limit cycle. Then each point on the cycle corresponds to a certain value of the phase. Note that the phase is defined to grow uniformly in time, while the system may not evolve uniformly along the limit cycle (it may go faster in phase space in some places on the cycle than others) [1, 34]. This idea of the phase of an oscillator will become important later in the Kuramoto model.

Also associated with each oscillator is its natural angular frequency, commonly called  $\omega$ . This quantity characterizes how quickly the oscillator travels around its limit cycle in the absence of outside influences. In



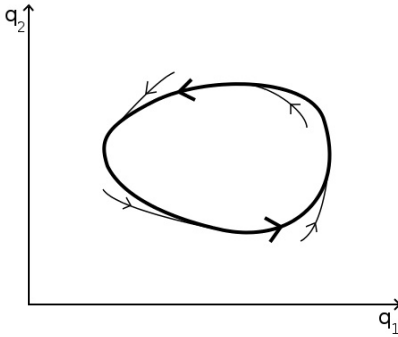


Figure 1.1: A limit cycle in phase space: The area of this plot is called a two-dimensional phase space. Any point in phase space corresponds to a different state of the system, which is defined in this case by two state variables  $q_1$  and  $q_2$ . Trajectories in phase space show how the system evolves in time. The bold curve is a closed limit cycle; on this curve, the system repeats the same behavior over and over indefinitely. Notice that all trajectories near the limit cycle approach the limit cycle — i.e. the cycle is stable. This type of limit cycle corresponds to a self-sustained oscillator.

other words,  $\omega$  is the rate of change of the oscillator's phase when it is alone.

Besides self-sustained oscillators, it is worth noting one other category of systems called rotators. This group includes such systems as rotating pendula and Josephson junctions. Rotators cannot be called self-sustained oscillators because they require an external energy source in order to oscillate (whereas a self-sustained oscillator is powered by an intrinsic, internal energy source). Even so, they still exhibit much of the same behavior of self-sustained oscillators since they have a stable limit cycle [1, 114-116]. In the case of rotators, there is already a well-defined phase (a pendulum's phase, for example, can be defined as the angle it makes with some axis), so this is used instead of the uniformly growing phase of self-sustained oscillators. Other than this difference in mathematical terminology, as far as synchronization is concerned, the properties of rotators and self-sustained oscillators are nearly the same.

With this mathematical background, we are ready to look at the main topic of my project, the Kuramoto Model.

## 1.5 The Kuramoto Model

In the 1960s, due to the prevalence of the somewhat mysterious phenomenon of collective synchronization in so many different natural systems, various scientists began to work on a mathematical model for this behavior. In particular, Arthur Winfree pioneered a method that has since become very popular. Winfree looked at the behavior of a large collection of interacting limit-cycle oscillators, in an attempt to model

collective synchronization in large groups, like the example of the flashing fireflies. He constructed his model by assuming 1) that the oscillators are nearly identical, and 2) that the coupling among oscillators is small. These assumptions helped simplify the math tremendously, by allowing for the separation of slow and fast timescales. On a fast timescale, the oscillators quickly relax to their limit cycles since the perturbations from the other oscillators are small; because it never gets far from the limit cycle, each oscillator's state can be approximated well by just its phase. Then on a slower timescale, one can talk about how the phase of each oscillator is changing due to the effects of the other oscillators. This made the math much easier, because the only variable to keep track of was the phase of each oscillator, as opposed to all of its state variables [4, 2].

Winfree went on to propose a model in which the effect on each oscillator's phase is determined by the combined state of all of the oscillators (known as a mean-field approximation). In his model, the rate of change of the phase of an oscillator is determined by a combination of its natural frequency  $\omega_i$  and the collective state of all of the oscillators combined. Each oscillator's sensitivity to the collective rhythm is determined by a function  $Z$ , and its own contribution to the collective rhythm is specified by a function  $X$ . Thus each oscillator has an equation describing how its phase changes in time:

$$\dot{\theta}_i = \omega_i + \left( \sum_{j=1}^N X(\theta_j) \right) Z(\theta_i), \quad i = 1, \dots, N, \quad (1.1)$$

where  $\theta_i$  is the phase of oscillator  $i$ ,  $\dot{\theta}_i$  is the rate of change of the phase of oscillator  $i$ ,  $\omega_i$  is the natural frequency of oscillator  $i$ , and  $N$  is the total number of oscillators [4, 2].

Winfree studied this model with computer simulations and analytical approximations and found that the oscillators could indeed synchronize given a sufficiently large coupling and a sufficiently small detuning (range of natural frequencies). He found an even more interesting result by setting the detuning to a high value (so the oscillators could not synchronize), and then slowly lowering it. The unsynchronized incoherence would always continue until a certain threshold, when a group of oscillators would suddenly jump into synchrony. It seemed that the population was experiencing a phase transition, with groups freezing into synchrony much like water turns to ice [4, 2].

Yoshiki Kuramoto was intrigued by Winfree's results, and he began working with collective synchronization in 1975. He used the same assumptions that Winfree proposed, and after some intensive mathematical averaging, he proved that the long-term dynamics of any system of nearly identical, weakly coupled limit-

cycle oscillators can be described by the following equation [4, 3][5]:

$$\dot{\theta}_i = \omega_i + \sum_{j=1}^N \Gamma_{ij}(\theta_j - \theta_i), \quad i = 1, \dots, N, \quad (1.2)$$

where the interaction function  $\Gamma_{ij}$  determines the form of coupling between oscillator  $i$  and oscillator  $j$ .

This is a very general equation, allowing for any kind of coupling. Even with the simplification that this phase model presents, the interaction functions  $\Gamma_{ij}$  can be hard to analyze in general, so there is not a lot that can be done theoretically from here.

But Kuramoto continued to work with his model, and he took a similar step to Winfree's and assumed that each oscillator affected every other oscillator. This kind of interaction is called global coupling. He further assumed that the interactions were equally weighted and depended only sinusoidally on the phase difference. This gave interaction functions

$$\Gamma_{ij}(\theta_j - \theta_i) = \frac{K}{N} \sin(\theta_j - \theta_i), \quad (1.3)$$

producing the governing equations of what has come to be known as the Kuramoto Model:

$$\dot{\theta}_i = \omega_i + \frac{K}{N} \sum_{j=1}^N \sin(\theta_j - \theta_i), \quad i = 1, \dots, N, \quad (1.4)$$

where  $K$  is the coupling constant, and  $N$  is the total number of oscillators. The model is often used as  $N \rightarrow \infty$ , so the  $1/N$  factor is present to keep the model well-behaved in this limit.

For simplicity in theoretical calculations, the natural frequencies  $\omega_i$  are generally distributed according to a probability density  $g(\omega)$  that is symmetric about some frequency  $\Omega$ , so that  $g(\Omega + \omega) = g(\Omega - \omega)$ . A Gaussian distribution is often used, for example. To further simplify, the mean frequency  $\Omega$  can be moved to 0 by making the shift  $\theta_i \rightarrow \theta_i + \Omega t$ . This is the same as working in a frame rotating at the mean frequency  $\Omega$ . The equations remain the same and there is the added simplification that  $g(\omega) = g(-\omega)$ . It is also normally assumed that  $g(\omega)$  decreases monotonically on each side from the peak at  $\omega = 0$  [4, 3].

What makes the Kuramoto Model so interesting is the theoretical work that can be done with it. With a few more mathematical steps, Kuramoto was not only able to prove that there will be a phase transition to synchronization with his model, but also to find a direct equation that gives the critical coupling strength necessary for synchronization [5]. It is equally amazing that, even with all the simplifications that Kuramoto made to create his model, it has been found to work in describing some synchronizing systems. One shining

example of this is a series array of Josephson junctions<sup>2</sup>, which has been shown theoretically to be completely equivalent to the Kuramoto model for small coupling [1, 291-294]. In addition, in [6], Kiss *et al.* have recently presented the first experimental evidence of a physical system mapping to the Kuramoto model, using populations of precisely controllable chemical oscillators to confirm that the model correctly predicts the conditions required for synchronization.

In my research, I first retraced Kuramoto's initial steps in the formulation and theoretical analysis of his model, including, for example, the calculation of the critical coupling strength required for synchronization. This, along with the results of initial numerical simulations, makes up Chapter 2. From there, I studied how noise can be added to the system (Chapter 3) and how mathematics can be used to analyze the behavior of the system with noise (Chapter 4). Numerical simulations were run for the noisy case as well.

---

<sup>2</sup>Also see [7] for our previous work on a similar problem, in which a ladder array of Josephson junctions is mapped onto a locally coupled Kuramoto model.

## Chapter 2

# Kuramoto's Model of Coupled, Nonlinear Oscillators

### 2.1 Solving for $K_C$

The most striking point in Kuramoto's original analysis of his model (see [5]) was his ability to solve exactly for the critical coupling needed for synchronization. Here we retrace his steps (following [4]) in producing this important result.

#### 2.1.1 Mean-Field Parameters

The first step is to recast the governing equations (1.4) of the model in terms of the following order parameter:

$$re^{i\psi} = \frac{1}{N} \sum_{j=1}^N e^{i\theta_j}. \quad (2.1)$$

The modulus of the order parameter,  $r$ , is a measure of the amount of collective behavior in the system, and the phase  $\psi$  gives the average phase of all the oscillators. We say that the order parameter describes the “mean field” of the system. A good way to visualize this idea is to imagine each oscillator as a point moving around the unit circle. Then the order parameter could be imagined as an arrow pointing from the center of the circle as shown in Fig. 2.1.

To write the governing equations in terms of the order parameter, first multiply both sides of Eq. (2.1)

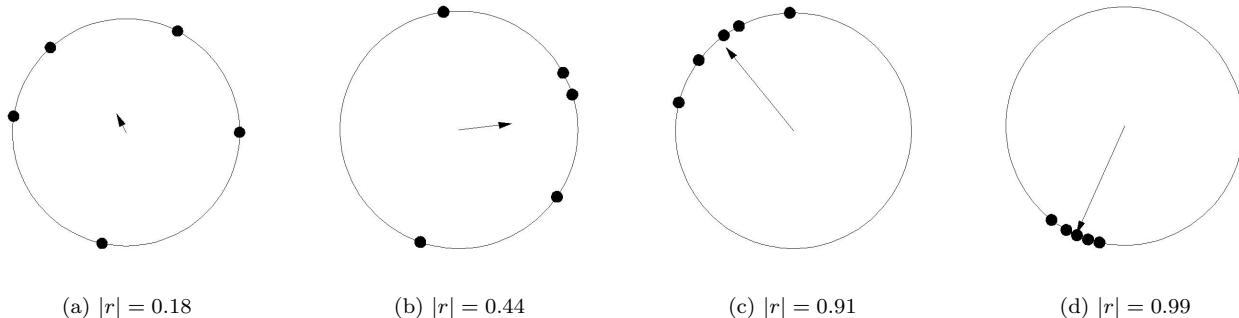


Figure 2.1: The order parameter is represented by the vector pointing from the center of the unit circle. Notice that the length of the order parameter increases as the phases of the oscillators get closer together.

by  $e^{i\theta_i}$  to get

$$r e^{i(\psi - \theta_i)} = \frac{1}{N} \sum_{j=1}^N e^{i(\theta_j - \theta_i)}, \quad i = 1, \dots, N, \quad (2.2)$$

whose imaginary parts are

$$r \sin(\psi - \theta_i) = \frac{1}{N} \sum_{j=1}^N \sin(\theta_j - \theta_i), \quad i = 1, \dots, N. \quad (2.3)$$

This can be substituted into Eq. (1.4) to obtain the governing equations in terms of the order parameter:

$$\dot{\theta}_i = \omega_i + K r \sin(\psi - \theta_i), \quad i = 1, \dots, N. \quad (2.4)$$

Note that the interactions between the individual oscillators can thus be described solely through the mean-field quantities  $r$  and  $\psi$ . The coupling term says that the phase of each oscillator is pulled toward the average phase of the whole ensemble, with a strength proportional to the magnitude of the order parameter. This way of looking at the problem greatly simplifies how we can think about synchronization.

### 2.1.2 Steady Solutions

The other key simplification we make in search of synchronization is to look only at steady states, where  $r(t)$  is time independent and  $\psi(t)$  rotates uniformly at an angular frequency  $\Omega$ . Thus we are looking for states of the system when any transient behavior has died off and the order parameter is of constant length and rotating at a constant frequency. If we also go into a frame of reference that is rotating at the same frequency  $\Omega$ , then  $r(t)$  will be completely stationary, and we can set  $\psi(t)$  to some arbitrary constant value;

so we will say  $\psi(t) \equiv 0$  in the rotating frame. In Figure 2.1, this corresponds to a configuration where the order parameter vector is not rotating or changing in length.

In this case, the governing equations (2.4) become

$$\dot{\theta}_i = \omega_i - Kr \sin \theta_i, \quad i = 1, \dots, N. \quad (\text{rotating frame}) \quad (2.5)$$

From this equation, since  $\sin \theta_i \leq 1$ , we see that oscillators with natural frequencies<sup>1</sup>  $|\omega_i| \leq Kr$  can have a static solution  $\dot{\theta}_i = 0$  when

$$\omega_i = Kr \sin \theta_i. \quad (2.6)$$

Oscillators in this state are frequency locked since they are all stationary in the rotating frame. It is possible to solve for the phase angle  $\theta_i$  at which they lock using Eq. (2.6). The oscillators with natural frequencies  $|\omega_i| > Kr$  will not be able to frequency lock ( $\dot{\theta}_i \neq 0$ ), so they move around the unit circle in a nonuniform manner. In terms of Figure 2.1, then, there are some oscillators that are locked in one position, but there are also unsynchronized oscillators drifting around.

Even with these drifting oscillators, we still want to assume that  $r$  and  $\psi$  are constant to find the steady state solutions. To achieve this, we force the *distribution* of oscillators around the circle to be time independent, even if the individual oscillators are moving. To ensure that the distribution remains constant in time, we force it to be inversely proportional to the oscillators' speed at  $\theta$ —in an area where there are fewer oscillators, they must be going faster, to keep the same number of oscillators in that area. Thus we define the density of oscillators as follows, a function of angular frequency  $\omega$  and angular position  $\theta$  on the unit circle:

$$\rho(\theta, \omega) = \frac{C}{|\dot{\theta}|} = \frac{C}{|\omega - Kr \sin \theta|}, \quad (2.7)$$

where  $\rho(\theta, \omega)d\theta$  gives the fraction of oscillators with angular frequency  $\omega$  that are found between  $\theta$  and  $\theta + d\theta$ .  $C$  is a constant that can be found through normalization:

$$1 = \int_{-\pi}^{\pi} \rho(\theta, \omega) d\theta = C \int_{-\pi}^{\pi} \frac{d\theta}{|\omega - Kr \sin \theta|}, \quad (2.8)$$

which gives

$$C = \frac{1}{2\pi} \sqrt{\omega^2 - (Kr)^2}. \quad (2.9)$$

---

<sup>1</sup>The natural frequencies are allowed to be positive or negative, corresponding to oscillations in opposite directions along the limit cycle.

### 2.1.3 Solving for the Order Parameter and $K_C$

In Section 2.1.2, we identified two distinct groups of oscillators: those that are frequency locked and those that are drifting. This means that when we are solving for the order parameter [using Eq. (2.1)], we can split up the sum into two parts. Also notice that since we are in the rotating frame,  $\psi = 0$ , so the order parameter  $r e^{i\psi} = r e^0 = r$ . Then  $r$  must equal the sum of the average order parameter of the locked oscillators and the average order parameter of the drifting oscillators [based on Eq. (2.1)]:

$$r = \langle e^{i\theta} \rangle_{\text{lock}} + \langle e^{i\theta} \rangle_{\text{drift}}, \quad (2.10)$$

where the nature of the averaging process is described below.

First we solve for the contribution to  $r$  due to the drifting oscillators. To do this, we integrate the distribution  $\rho(\theta, \omega)$  over the whole circle and for all oscillators that are not frequency locked ( $\omega > Kr$ ), multiplying by the contribution  $e^{i\theta}$  to the order parameter:

$$\langle e^{i\theta} \rangle_{\text{drift}} = \int_{-\pi}^{\pi} \int_{|\omega| > Kr} e^{i\theta} \rho(\theta, \omega) g(\omega) d\omega d\theta. \quad (2.11)$$

Notice in Eq. (2.7) that  $\rho(\theta + \pi, -\omega) = \rho(\theta, \omega)$ , and also remember that we defined  $g$  so that  $g(-\omega) = g(\omega)$ . These symmetries make the integral for the positive values of  $\omega$  cancel with that of the negative values, making the integral vanish (see Appendix A for details). So we have

$$\langle e^{i\theta} \rangle_{\text{drift}} = 0. \quad (2.12)$$

Therefore the locked oscillators are the only contributors to the order parameter—the drifting oscillators cancel each other out. This is intuitively plausible because there is no preferred value of  $\theta$  or direction of rotation for these oscillators.

Now we just need to solve for the locked oscillators' contribution. First, we know from Eq. (2.6) that  $\sin \theta_i = \omega_i / Kr$ . Then, since  $g(\omega)$  is centered at zero and defined to be even, the phases  $\theta_i$  of the locked oscillators will also be centered symmetrically on zero, meaning  $\langle \sin \theta \rangle_{\text{lock}} = 0$ . So we are left with only the cosine part of the complex exponential:

$$r = \langle e^{i\theta} \rangle_{\text{lock}} = \langle \cos \theta \rangle_{\text{lock}} = \int_{-Kr}^{Kr} \cos[\theta(\omega)] g(\omega) d\omega, \quad (2.13)$$



where  $\theta(\omega)$  is defined by Eq. (2.6). Now we use Eq. (2.6) to change the variables from  $\omega$  to  $\theta$ :

$$r = \int_{-\frac{\pi}{2}}^{\frac{\pi}{2}} \cos \theta g(Kr \sin \theta) Kr \cos \theta d\theta = Kr \int_{-\frac{\pi}{2}}^{\frac{\pi}{2}} \cos^2 \theta g(Kr \sin \theta) d\theta. \quad (2.14)$$

This equation defines solutions that satisfy our initial constraint that the order parameter be constant.

First,  $r = 0$  is always a solution. This is the completely incoherent state, meaning that there is no synchronization. Solving for the distribution in this case using Eq. (2.7), we get  $\rho(\theta, \omega) = \frac{1}{2\pi}$ , a constant, meaning that you are equally likely to find an oscillator anywhere on the circle.

The solutions corresponding to nonzero  $r$  are states in which there is a nonzero set of oscillators that are fully frequency locked but (for  $r < 1$ ) only partially phase locked. Dividing Eq. (2.14) by  $r$ , these states are solutions to

$$1 = K \int_{-\frac{\pi}{2}}^{\frac{\pi}{2}} \cos^2 \theta g(Kr \sin \theta) d\theta. \quad (2.15)$$

If we let  $r \rightarrow 0^+$  in this equation, we are finding the critical point  $K_C$  at which the order parameter rises from zero. When we do this, Eq. (2.15) becomes

$$1 = K_C \int_{-\frac{\pi}{2}}^{\frac{\pi}{2}} \cos^2 \theta g(0) d\theta = K_C g(0) \int_{-\frac{\pi}{2}}^{\frac{\pi}{2}} \cos^2 \theta d\theta = K_C g(0) \frac{\pi}{2}. \quad (2.16)$$

Solving for  $K_C$ , we have

$$K_C = \frac{2}{\pi g(0)}. \quad (2.17)$$

This is exactly what we were looking for— $K_C$  is the critical value of the coupling required to produce a partially phase-synchronized state.

## 2.2 The Growing Order Parameter

Now that we know where the order parameter  $r$  first rises from zero, we are interested to know how  $r$  grows as the coupling  $K$  increases further, i.e. for  $K > K_C$ .

### 2.2.1 Initial Growth

To discover how  $r$  behaves close to  $K_C$ , we can expand  $g(Kr \sin \theta)$  in Eq. (2.15) about  $r = 0$ :

$$g(Kr \sin \theta) \approx g(0) + g'(0)Kr \sin \theta + \frac{1}{2}g''(0)(Kr \sin \theta)^2. \quad (2.18)$$

Since we know  $g(\omega)$  has a maximum at zero,  $g'(0) = 0$ , so

$$g(Kr \sin \theta) \approx g(0) + \frac{1}{2}g''(0)(Kr \sin \theta)^2. \quad (2.19)$$

Substituting this back into Eq. (2.15), we get

$$1 = K \int_{-\frac{\pi}{2}}^{\frac{\pi}{2}} \cos^2 \theta \left[ g(0) + \frac{1}{2}g''(0)(Kr \sin \theta)^2 \right] d\theta \quad (2.20)$$

Performing the integral and making use of Eq. (2.17) gives

$$1 = K \left[ g(0) \frac{\pi}{2} + \frac{K^3 r^2 g''(0) \pi}{2 \cdot 8} \right] = \frac{K}{K_C} + \frac{\pi K^3 r^2 g''(0)}{16}. \quad (2.21)$$

Now multiply through by  $K_C$ , and since we are assuming  $K \approx K_C$ , then  $K^3 \approx K_C^3$ :

$$K_C = K + K_C \frac{\pi K_C^3 r^2 g''(0)}{16}. \quad (2.22)$$

We now solve for the scaled distance from the critical point, generally called  $\mu$ :

$$\mu \equiv \frac{K - K_C}{K_C} = \frac{-\pi K_C^3 r^2 g''(0)}{16}. \quad (2.23)$$

Then we can solve for the order parameter  $r$ :

$$r = \sqrt{\frac{-16\mu}{\pi g''(0) K_C^3}}, \quad (2.24)$$

or equivalently,

$$r = \sqrt{\frac{-16}{\pi g''(0) K_C^4} (K - K_C)^{1/2}}. \quad (2.25)$$

Thus, near the critical point,  $r$  is proportional to the square root of the distance from  $K_C$ .

This is as much as we can know unless we have the exact form of the distribution of natural frequencies  $g(\omega)$ . Even then, it is most often impossible to solve for  $r(K)$  explicitly.

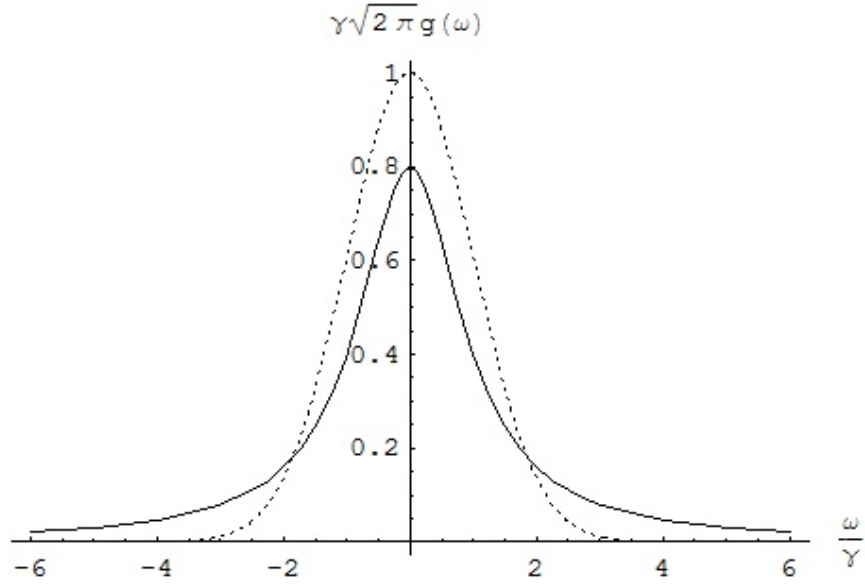


Figure 2.2: The solid line is a Lorentzian distribution of width  $\gamma$  in unitless variables. A Gaussian distribution of width  $\gamma$  is shown as a dotted line for comparison. Notice that the Lorentzian has characteristically large “tails.”

### 2.2.2 Lorentzian density

Kuramoto, however, discovered a special case in which it is possible to solve explicitly for  $r(K)$ . He used a Lorentzian density, defined as

$$g(\omega) = \frac{\gamma}{\pi(\gamma^2 + \omega^2)}, \quad (2.26)$$

where  $\gamma$  is a constant defining the width of the distribution. Figure 2.2 shows a Lorentzian distribution along with a Gaussian distribution for comparison. It turns out that substituting the Lorentzian distribution (2.26) into Eq. (2.15) produces a solvable integral. The end result for the order parameter is

$$r = \sqrt{1 - \frac{2\gamma}{K}}, \quad (2.27)$$

or, since we know that

$$K_C = \frac{2}{\pi g(0)} = \frac{2}{\pi \frac{1}{\pi\gamma}} = 2\gamma, \quad (2.28)$$

$$r = \sqrt{1 - \frac{K_C}{K}}. \quad (2.29)$$

A plot of this function is shown as the solid line in Figure 2.3 in the next section. The order parameter rises from zero at  $K_C$  and then asymptotically approaches 1 as  $K$  increases.

## 2.3 Numerical Simulations

Numerical simulations of the Kuramoto model were run to get a feel for how the results change when including only a finite number of oscillators and to ensure that our simulations were working correctly before we started adding noise. A computer program was run that simulates a large number of oscillators<sup>2</sup> that interact according to Eq. (2.4). The natural frequencies were selected randomly according to a Lorentzian distribution  $g(\omega)$ , and the initial phases were selected randomly around the unit circle. The program then allowed the system to evolve over small discrete timesteps, using a fourth-order Runge-Kutta method to simulate the nonlinear equations given in Eq. (2.4).

After a sufficient number of timesteps had passed so that any transient behavior had died out (we used 500,000 timesteps), various properties of the system were recorded to determine the amount of synchronization that had occurred. For example, the magnitude of the order parameter  $|r|$  gives information about how fully the oscillators are phase synchronized—if  $|r| = 0$ , the oscillators are spread uniformly around the unit circle, and if  $|r| = 1$ , all the oscillators are exactly phase-locked. Figure 2.3 shows how  $|r|$  increases as the coupling  $K$  between the oscillators is increased. The theoretical calculation of  $|r|$  as a function of  $K$  is given by Eq. (2.29), and is plotted along with the numerical results for comparison.

Two other ways of visualizing the synchronization are shown in Figures 2.4 and 2.5.<sup>3</sup> These figures show the results after the same type of simulation, but here the phase  $\theta_n$  and the angular speed  $\Omega_n$  for each oscillator are shown. The values in each plot are arranged from lowest to highest natural oscillator frequency, and three plots are given in each figure to show the effect of changing the coupling constant  $K$  from below to above  $K_C = 1$ . In Figure 2.4, we see how the phases of the oscillators are first distributed randomly when  $K < K_C$ , and then start to group together when  $K \geq K_C$ . This shows the start of phase synchronization. In Figure 2.5, the angular speeds are close to their natural values when  $K < K_C$ , but when  $K \geq K_C$ , oscillators with natural frequencies close to zero begin to synchronize to have an angular speed of exactly zero. This shows the start of frequency synchronization.

---

<sup>2</sup> $N$  typically varied from 200 to 1000.

<sup>3</sup>The form of these figures is taken from [1, 284], but they display the data we collected.

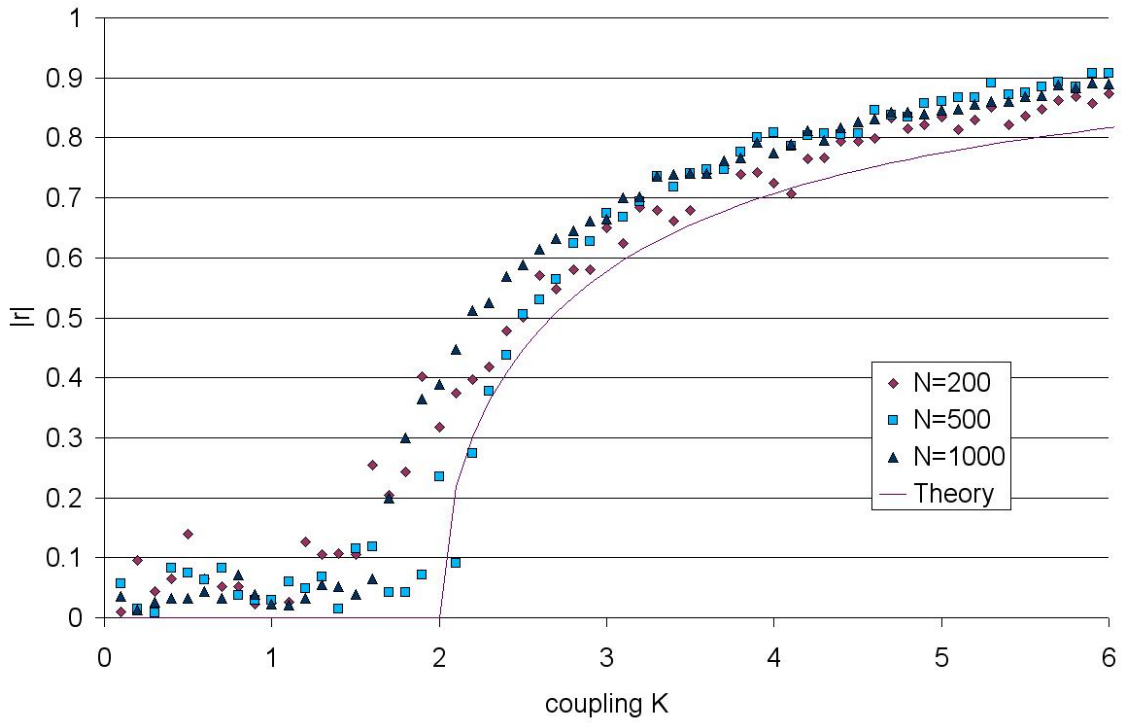


Figure 2.3: This plot shows how the magnitude of the order parameter  $|r|$ , which indicates the degree of phase synchronization, rises as the coupling  $K$  between oscillators is increased. Numerical results are shown as symbols, and are taken from the simulation of  $N$  oscillators with natural frequencies distributed randomly according to a Lorentzian distribution. The solid line shows the theoretical curve for a Lorentzian distribution given by Eq. (2.29).

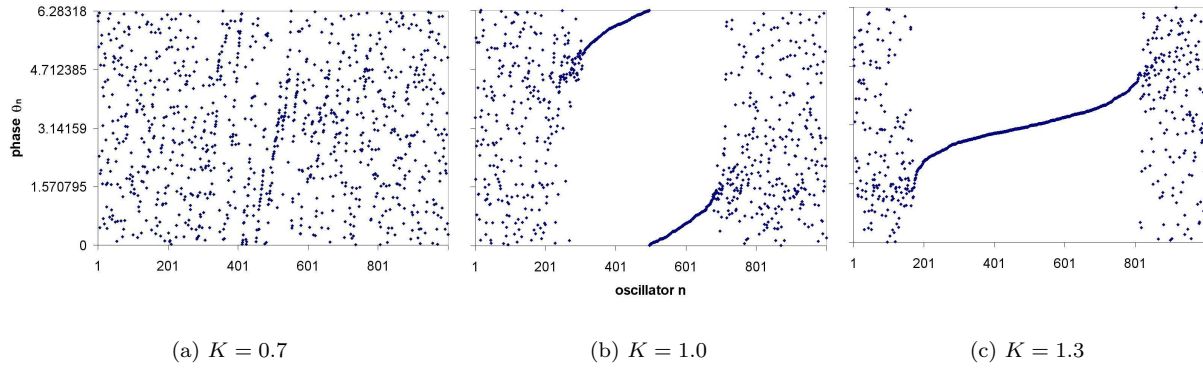


Figure 2.4: The phase  $\theta_n$  of each of 1000 oscillators in a simulation of the Kuramoto model, with varying values for the coupling constant  $K$ . The oscillators are numbered from lowest to highest natural frequency, with natural frequencies selected according to a Lorentzian distribution with  $\gamma = 0.5$ . From Eq. (2.28),  $K_C = 1$ . Partial phase synchronization is visible at and above  $K_C$ .

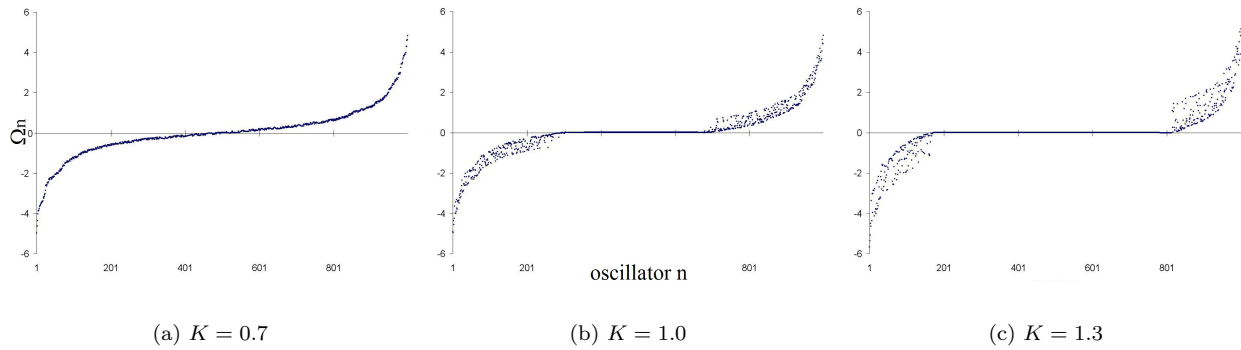


Figure 2.5: The angular speed  $\Omega_n$  of each of 1000 oscillators in a simulation of the Kuramoto model, with varying values for the coupling constant  $K$ . The oscillators are numbered from lowest to highest natural frequency, with natural frequencies selected according to a Lorentzian distribution with  $\gamma = 0.5$ . From Eq. (2.28),  $K_C = 1$ . Partial frequency synchronization is visible at and above  $K_C$ .

## Chapter 3

# Adding Noise to the Kuramoto Model

Noise is usually present in any physical system — as one example, the behavior of an array of Josephson junctions could be greatly affected by thermal noise — so it is important to study how random noise can change the synchronization behavior seen in the Kuramoto model. In this chapter we study how noise is added to the model, and in the next chapter we analyze its effects.

### 3.1 An Example of a Stochastic Process

Before adding noise to the Kuramoto model, it is useful to step back and look at how a simpler stochastic (random) process works. Here we study the Wiener process, defined so that if  $X$  represents the position of a particle along an axis, the particle will demonstrate a jittery “random walk” along the axis as time goes on. The process is described mathematically by Eq. (3.1), called an update equation because if you know the position of the particle at a certain time  $t$ , the equation tells you how to find the position a short time  $dt$  later:

$$X(t + dt) = X(t) + \sqrt{\delta^2 dt} N(0, 1), \quad (3.1)$$

where  $\delta$  defines the strength of the noise in the system and  $N(0, 1)$  represents a random number chosen from a normal (Gaussian) distribution of mean 0 and variance 1 [8, 43-45].

Another equally valid way exists for describing the Wiener process. Instead of tracking a single particle’s movement, for which the update equation was designed, we can look at a probability density  $\rho(x, t)$  for a large number of such particles that describes the probability of finding a particle at a certain location and time. This density is defined so that  $\rho(x, t)dx$  gives the probability of finding a particle between  $x$  and  $x + dx$

at time  $t$ . Using properties of normal random variables, we express the Wiener process as

$$X(t) = X(0) + N(0, \delta^2 t), \quad (3.2)$$

where  $N(0, \delta^2 t)$  represents a normal random variable with mean 0 and variance  $\delta^2 t$ . Notice that as time goes on, the width of the normal distribution increases, meaning you are more likely to find particles further away from the starting point. Figure 3.1 shows this spreading of the density function  $\rho$  [8, 45-46].

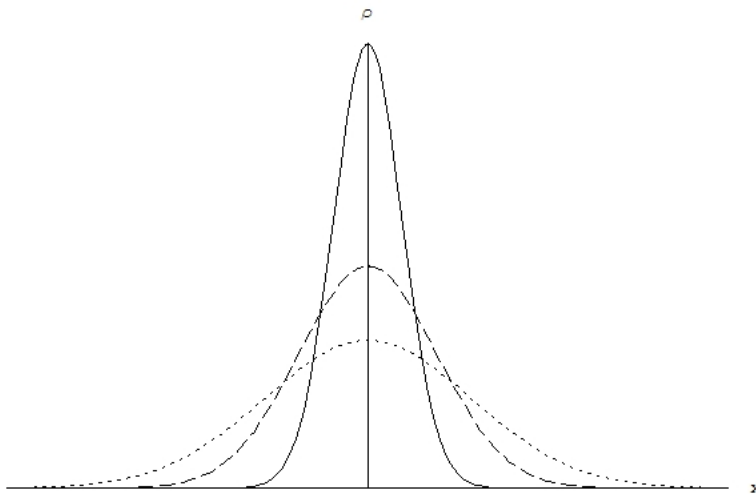


Figure 3.1: The spreading of the probability density function under the Wiener process. The solid line is at  $t = 1$ , the dashed line is at  $t = 2$ , and the dotted line is at  $t = 3$  (with arbitrary units).

In fact, this spreading of the probability density satisfies the classical diffusion equation

$$\frac{\partial \rho(x, t)}{\partial t} = \frac{\delta^2}{2} \frac{\partial^2 \rho(x, t)}{\partial x^2}. \quad (3.3)$$

If you start with an initial probability function representing the distribution of the particles, Eq. (3.3) describes how the density will evolve under the Wiener process. Thus the process can be fully described either in the update equation form [Eq. (3.1)] or as an evolution equation [Eq. (3.3)] for a density function [8, 48-49]. Looking at a stochastic process in terms of the evolution of a density function turns out to be the most useful form when we take the Kuramoto model to the continuum limit.



## 3.2 The Continuum Limit<sup>1</sup>

When including noise, it is useful mathematically to let the number of oscillators go to infinity. Once there are an infinite number of oscillators, instead of keeping track of the phase of each individual oscillator, it is convenient to describe the system in terms of a density function. Now we see the system as a continuum (a continuous “fluid”) of oscillators, and we talk only in terms of the density of oscillators at different locations on the unit circle (see Fig. 3.2).

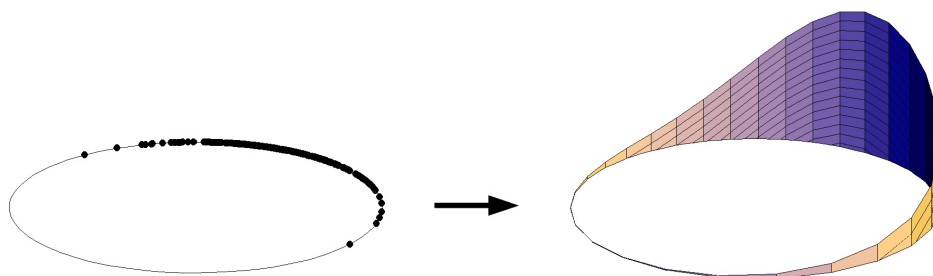


Figure 3.2: The continuum limit: As the number of oscillators goes to infinity, instead of tracking individual oscillators (on the left), we describe the system with a continuous density function (on the right) that gives the density of oscillators at each point around the unit circle.

Mathematically, the density function  $\rho(\theta, \omega, t)$  is defined similarly to  $\rho(x, t)$  in the previous section, but now  $\rho(\theta, \omega, t)d\theta$  gives the fraction of oscillators with natural frequency  $\omega$  that lie between  $\theta$  and  $\theta + d\theta$  at time  $t$ . It is normalized so that

$$\int_0^{2\pi} \rho(\theta, \omega, t) d\theta = 1 \quad (3.4)$$

for all values of  $t$  and  $\omega$ . It must also satisfy the following continuity equation:

$$\frac{\partial \rho}{\partial t} = -\frac{\partial}{\partial \theta}(\rho v). \quad (3.5)$$

This condition ensures conservation of oscillators: it essentially says that if the density is increasing in a certain region (see left-hand side), then there must be a corresponding flow into the region from somewhere else (meaning the velocity of the oscillators is decreasing as you move into the area; see right-hand side). Armed with this information, we can recast the Kuramoto model equations in terms of the density function  $\rho$ .

---

<sup>1</sup>This section follows section 7 in [4].

First, we know from Eq. (2.4) that the (instantaneous) velocity of each oscillator is given by

$$v(\theta, t, \omega) = \omega + Kr \sin(\psi - \theta) = \omega + Kr(\sin \psi \cos \theta - \cos \psi \sin \theta). \quad (3.6)$$

Inserting Eq. (3.6) into Eq. (3.5) gives

$$\frac{\partial \rho}{\partial t} = -\frac{\partial}{\partial \theta} [\rho \cdot [\omega + Kr(\sin \psi \cos \theta - \cos \psi \sin \theta)]]. \quad (3.7)$$

To get  $r$  and  $\psi$ , we take Eq. (2.1) to the continuum limit  $N \rightarrow \infty$  using our densities  $\rho$  and  $g$ :

$$r e^{i\psi} = \int_0^{2\pi} \int_{-\infty}^{\infty} e^{i\theta'} \rho(\theta', t, \omega') g(\omega') d\omega' d\theta', \quad (3.8)$$

which tells us that

$$r \cos \psi = \int_0^{2\pi} \int_{-\infty}^{\infty} \cos \theta' \rho(\theta', t, \omega') g(\omega') d\omega' d\theta' \quad (3.9)$$

$$r \sin \psi = \int_0^{2\pi} \int_{-\infty}^{\infty} \sin \theta' \rho(\theta', t, \omega') g(\omega') d\omega' d\theta'. \quad (3.10)$$

These are substituted into Eq. (3.7) to give

$$\begin{aligned} \frac{\partial \rho}{\partial t} = -\frac{\partial}{\partial \theta} \left[ \rho \left( \omega + K \cos \theta \int_0^{2\pi} \int_{-\infty}^{\infty} \cos \theta' \rho(\theta', t, \omega') g(\omega') d\omega' d\theta' \right. \right. \\ \left. \left. - K \sin \theta \int_0^{2\pi} \int_{-\infty}^{\infty} \sin \theta' \rho(\theta', t, \omega') g(\omega') d\omega' d\theta' \right) \right], \end{aligned} \quad (3.11)$$

which is equivalent to

$$\frac{\partial \rho}{\partial t} = -\frac{\partial}{\partial \theta} \left[ \rho \left( \omega + K \int_0^{2\pi} \int_{-\infty}^{\infty} \sin(\theta' - \theta) \rho(\theta', t, \omega') g(\omega') d\omega' d\theta' \right) \right]. \quad (3.12)$$

Equation (3.12) is the Kuramoto model in the continuum limit. Although this seems to just make things more complicated (we are now faced with a nonlinear partial integro-differential equation), this formulation gives us a framework for adding noise to the system.

To check that we can still derive the same results as Section 2.1.2, we again look at the stationary states, this time by setting  $\partial \rho / \partial t = 0$ . From Eq. (3.5) we see that this forces  $\rho v = C(\omega)$ , where  $C(\omega)$  is constant with respect to  $\theta$ .

If  $C(\omega) \neq 0$ , then we solve for  $\rho$  to write

$$\rho = \frac{C(\omega)}{v} = \frac{C(\omega)}{\omega + Kr \sin(\psi - \theta)}, \quad (3.13)$$

which matches with the density equation (2.7) that we found earlier for the drifting oscillators.

If  $C(\omega) = 0$ , in order for  $\rho$  to be normalizable, it must be that  $\rho$  is a delta function, peaked at some  $\theta'$ :

$$C(\omega) = \rho v = \delta(\theta - \theta') v = \delta(\theta - \theta') (\omega - Kr \sin \theta) = 0. \quad (3.14)$$

Integrate with respect to  $\theta$  to find:

$$\omega - Kr \sin \theta' = 0, \quad (3.15)$$

which matches with the locked oscillators and Eq. (2.6).

### 3.3 Adding Noise to the Kuramoto Model

Our goal is to find an equation that describes the evolution of the oscillator density function in the presence of noise. This will provide a starting point for analyzing how the behavior of the Kuramoto model changes when noise is added.

We begin by adding a noise term  $\xi$  to the Kuramoto equations in the discrete form (2.4) :

$$\dot{\theta}_i = \omega_i + \xi_i + Kr \sin(\psi - \theta_i), \quad i = 1, \dots, N, \quad (3.16)$$

where the noise term  $\xi_i$  is defined so that

$$\langle \xi_i(t) \rangle = 0 \quad (3.17)$$

$$\langle \xi_i(s) \xi_j(t) \rangle = 2D \delta_{ij} \delta(s - t). \quad (3.18)$$

The first condition means that the time average of the noise acting on oscillator  $i$  is zero, and the second requires that the noise terms for different oscillators or different times be non-correlated. The strength of the noise is set by the parameter  $D$ .

For running simulations of the Kuramoto model with noise, these equations are enough, since the noise term  $\xi$  can be simulated with a random number generator. To further study the model mathematically, however, we determine the evolution equation for the oscillator density function.

### 3.3.1 The Fokker-Planck Equation

Analogously to the Wiener process example given above, we can also express the Kuramoto model with noise in terms of the evolution of a density function. This will generalize Eq. (3.5) to include noise. This type of equation is called a Fokker-Planck equation.

The Fokker-Planck equation that describes the Kuramoto model is

$$\frac{\partial \rho}{\partial t} = D \frac{\partial^2 \rho}{\partial \theta^2} - \frac{\partial}{\partial \theta}(\rho v) \quad (3.19)$$

(see Appendix B for the derivation) [4]. Here  $D$  is the strength of the noise and  $v$  is given by Eq. (3.6). This equation tells us how the oscillator density function  $\rho(\theta, \omega, t)$  evolves in time, and is completely equivalent to the normal Kuramoto model equations with noise, Eq. (3.16). Notice that, although the derivation is not obvious, the equation makes some intuitive sense: the new first term is the diffusive part that tries to spread out the phases of the oscillators [compare with Eq. (3.3) for the Wiener process], and the second term is the continuity condition [as in Eq. (3.5)] that tries to synchronize the oscillators through the changing velocity  $v$ . We also get the expected result of Eq. (3.5) when we remove the noise by letting  $D \rightarrow 0$ .

The next step is to see how this Fokker-Planck equation behaves. Although it looks relatively simple, its complexity is hidden in the velocity  $v$ , which holds information about the oscillators' natural frequencies and how they are coupled. The next chapter reveals how we deal with this complexity and learn a surprising amount about the behavior of the system.

## Chapter 4

# The Effects of Noise: Stability

## Analysis

In this chapter<sup>1</sup>, to investigate the synchronization behavior of the Kuramoto model with noise, we look specifically at how the incoherent state (see Fig. 4.1) evolves in time, and in what situations it is stable. Since the incoherent state is defined so that the oscillators are distributed equally around the unit circle ( $r=0$ ), this corresponds to a completely unsynchronized state. If we find the situations in which this incoherent state just becomes unstable, we have found the situations where phase synchronization just starts to take place. In fact, we will find that this occurs at a certain coupling  $K_C$  just as in the noise-free case.

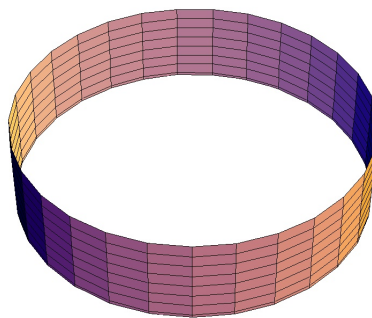


Figure 4.1: A representation of the incoherent state (see also Figure 3.2). The density of oscillators is constant over the unit circle, meaning you are equally likely to find oscillators at any point in their cycle. This corresponds to a completely unsynchronized state.

---

<sup>1</sup>Sections 4.1-4.3 follow section 3 in [11].

We study the stability of the incoherent state by adding a first order perturbation (i.e. giving the system a small “kick”) and noting whether the system returns to the incoherent state (in which case it is stable) or begins displaying some other kind of behavior (in which case it is unstable). The initial analysis is done to first order, dropping any terms that are multiplied by a small number squared. In the last part of my research, I attempted to extend this analysis to second order.

## 4.1 Adding a Perturbation

First, we add a small perturbation  $\eta$  to the incoherent state  $\rho(\theta, t, \omega) = 1/2\pi$ . We allow the perturbation to be an arbitrary function of  $\theta$ ,  $t$ , and  $\omega$ , and set its strength with a parameter  $\epsilon \ll 1$ :

$$\rho(\theta, t, \omega) = \frac{1}{2\pi} + \epsilon\eta(\theta, t, \omega). \quad (4.1)$$

Since we must still be able to normalize  $\rho$ , we require that

$$\int_0^{2\pi} \eta(\theta, t, \omega) d\theta = 0, \quad (4.2)$$

since the  $1/2\pi$  term already results in  $\int_0^{2\pi} \rho(\theta, t, \omega) d\theta = 1$ . Now we substitute this perturbed distribution into the Fokker-Planck equation (3.19) and find the first order  $[O(\epsilon)]$  approximation to find how  $\eta$  evolves. From the Fokker-Planck equation we have

$$\epsilon \frac{\partial \eta}{\partial t} = \epsilon D \frac{\partial^2 \eta}{\partial \theta^2} - \frac{\partial}{\partial \theta} \left[ \left( \frac{1}{2\pi} + \epsilon \eta \right) v \right]. \quad (4.3)$$

To find the  $O(\epsilon)$  contribution from what is in the square brackets, we need  $r$  so that we can find  $v$  from Eq. (2.4). So we substitute Eq. (4.1) into Eq. (3.8) to find

$$r e^{i\psi} = \int_0^{2\pi} \int_{-\infty}^{\infty} e^{i\theta} \left[ \frac{1}{2\pi} + \epsilon \eta \right] g(\omega) d\omega d\theta, \quad (4.4)$$

which can be simplified by noting that the  $e^{i\theta}/2\pi$  term will integrate to zero under the  $\theta$  integral, giving

$$r e^{i\psi} = \epsilon \int_0^{2\pi} \int_{-\infty}^{\infty} e^{i\theta} \eta(\theta, t, \omega) g(\omega) d\omega d\theta. \quad (4.5)$$

Notice that  $r$  is simply  $O(\epsilon)$ . We are actually looking for  $v$ , so if we define  $r_1$  as above, but factor out the  $\epsilon$ ,

$$r = \epsilon r_1, \quad (4.6)$$

then, by Eq. (2.4),  $v$  is given by

$$v = \omega + \epsilon K r_1 \sin(\psi - \theta). \quad (4.7)$$

We will also need the partial derivative of  $v$ :

$$\frac{\partial v}{\partial \theta} = -\epsilon K r_1 \cos(\psi - \theta). \quad (4.8)$$

Now we are ready to simplify Eq. (4.3). Its last term becomes

$$-\left(\frac{1}{2\pi} + \epsilon\eta\right) \frac{\partial v}{\partial \theta} - v \frac{\partial}{\partial \theta} \left(\frac{1}{2\pi} + \epsilon\eta\right), \quad (4.9)$$

which, when we substitute in for  $\partial v/\partial \theta$  from Eq. (4.8) and simplify, becomes

$$-\left(\frac{1}{2\pi} + \epsilon\eta\right) (-\epsilon K r_1 \cos(\psi - \theta)) - \epsilon v \frac{\partial \eta}{\partial \theta}. \quad (4.10)$$

Finally, when we substitute Eq. (4.7) for  $v$  and take only terms to  $O(\epsilon)$ , we end up with

$$\epsilon \frac{K}{2\pi} r_1 \cos(\psi - \theta) - \epsilon \omega \frac{\partial \eta}{\partial \theta}. \quad (4.11)$$

All of this is the last term of Eq. (4.3), so we put it back in and divide through by  $\epsilon$  to find the final equation that describes the evolution of the perturbation  $\eta$ :

$$\frac{\partial \eta}{\partial t} = D \frac{\partial^2 \eta}{\partial \theta^2} - \omega \frac{\partial \eta}{\partial \theta} + \frac{K}{2\pi} r_1 \cos(\psi - \theta). \quad (4.12)$$

This is the equation we will use to find the conditions under which  $\eta$  either dies off, in which case the incoherent state is stable, or grows, in which case the incoherent state is unstable.

## 4.2 Fourier Methods

To analyze the solutions of Eq. (4.12), we use Fourier methods. Specifically, we seek solutions of the form

$$\eta(\theta, t, \omega) = c(t, \omega)e^{i\theta} + c^*(t, \omega)e^{-i\theta} + \eta^\perp(\theta, t, \omega), \quad (4.13)$$

where  $c = c_1$  is the first Fourier coefficient in  $\eta$ 's expansion,  $c^* = c_1^*$  is its complex conjugate (since  $\eta$  is real,  $c_{-1} = c_1^*$ ), and  $\eta^\perp$  contains all the higher harmonics of  $\eta$ . We look for solutions this way since it turns out that only the first harmonic of  $\eta$  shows up in the expression for  $r$ , as shown below (and the order parameter  $r$  is all we really need to analyze the synchronization behavior). Note also that  $c_0$  does not show up because  $\eta$  has zero mean by Eq. (4.2).

We can see that  $r$  depends only on the first harmonic by substituting the Fourier series into Eq. (4.5):

$$\begin{aligned} r_1 e^{i\psi} &= \int_0^{2\pi} \int_{-\infty}^{\infty} e^{i\theta} \left( \sum_{n=-\infty}^{\infty} c_n(\omega, t) e^{in\theta} \right) g(\omega) d\omega d\theta \\ &= \int_{-\infty}^{\infty} \sum_n c_n(\omega, t) \left( \int_0^{2\pi} e^{i(1+n)\theta} d\theta \right) g(\omega) d\omega \\ &= \int_{-\infty}^{\infty} \sum_n c_n(\omega, t) 2\pi \delta_{n,-1} g(\omega) d\omega \\ &= 2\pi \int_{-\infty}^{\infty} c_{-1}(\omega, t) g(\omega) d\omega \\ &= 2\pi \int_{-\infty}^{\infty} c^*(\omega, t) g(\omega) d\omega. \end{aligned} \quad (4.14)$$

This means that we can solve for  $r(t)$  if we know only the first harmonic of  $\eta$ .

We use the result of Eq. (4.14) to express the last term of the evolution equation (4.12) in terms of  $c$  and  $c^*$ . First, note that

$$r_1 \cos(\psi - \theta) = \text{Re} [r_1 e^{i\psi} e^{-i\theta}]. \quad (4.15)$$

Then substitute Eq. (4.14), using the fact that  $\text{Re}(f) = (f + f^*)/2$ , to get

$$r_1 \cos(\psi - \theta) = \pi \left[ \left( \int_{-\infty}^{\infty} c^*(t, \omega) g(\omega) d\omega \right) e^{-i\theta} + \left( \int_{-\infty}^{\infty} c(t, \omega) g(\omega) d\omega \right) e^{i\theta} \right]. \quad (4.16)$$



Now we can write the evolution equation (4.12) in terms of  $c$  and  $c^*$  using Eqs. (4.13) and (4.16):

$$\begin{aligned} \frac{\partial}{\partial t} [ce^{i\theta} + c^*e^{-i\theta} + \eta^\perp] &= D \frac{\partial^2}{\partial \theta^2} [ce^{i\theta} + c^*e^{-i\theta} + \eta^\perp] - \omega \frac{\partial}{\partial \theta} [ce^{i\theta} + c^*e^{-i\theta} + \eta^\perp] \\ &+ \frac{K}{2\pi} \pi \left[ e^{-i\theta} \int_{-\infty}^{\infty} c^*g(\nu)d\nu + e^{i\theta} \int_{-\infty}^{\infty} cg(\nu)d\nu \right]. \end{aligned} \quad (4.17)$$

Taking the derivatives and collecting terms, we get

$$\begin{aligned} &e^{i\theta} \left[ \frac{\partial c}{\partial t} + Dc + i\omega c - \frac{K}{2} \int_{-\infty}^{\infty} cg(\nu)d\nu \right] \\ + &e^{-i\theta} \left[ \frac{\partial c^*}{\partial t} + Dc^* - i\omega c^* - \frac{K}{2} \int_{-\infty}^{\infty} c^*g(\nu)d\nu \right] \\ + &\left[ \frac{\partial \eta^\perp}{\partial t} - D \frac{\partial^2 \eta^\perp}{\partial \theta^2} + \omega \frac{\partial \eta^\perp}{\partial \theta} \right] = 0. \end{aligned} \quad (4.18)$$

Since this must hold for all values of  $\theta$ , each bracketed item must equal zero. The second bracket gives us no new information, since it is just the complex conjugate of the first. So we have separated the evolution equation into the following two equations, the first giving information about the fundamental harmonic, and the second for all the other harmonics:

$$\frac{\partial c}{\partial t} = -(D + i\omega)c + \frac{K}{2} \int_{-\infty}^{\infty} c(t, \nu)g(\nu)d\nu \quad (4.19)$$

$$\frac{\partial \eta^\perp}{\partial t} = D \frac{\partial^2 \eta^\perp}{\partial \theta^2} - \omega \frac{\partial \eta^\perp}{\partial \theta}. \quad (4.20)$$

First we will look at the evolution of the fundamental mode, since it is what determines  $r$ , which tells us about the synchronization behavior. Later we will look at the higher harmonics.

## 4.3 Evolution of the Fundamental Mode

### 4.3.1 Finding the Separable Solutions

In studying the evolution of the fundamental mode, we first look for separable solutions of Eq. (4.19) of the form

$$c(t, \omega) = b(\omega)e^{\lambda t}, \quad (4.21)$$

where the eigenvalue  $\lambda$  will tell us how  $c$  evolves in time. The linear operator  $L$  describing the right hand side of Eq. (4.19) is given by

$$Lc = -(D + i\omega)c + \frac{K}{2} \int_{-\infty}^{\infty} c(t, \nu)g(\nu)d\nu. \quad (4.22)$$

To solve for  $\lambda$ , we use the eigenvalue equation<sup>2</sup>

$$(L - \lambda I)c = (L - \lambda I)be^{\lambda t} = 0, \quad (4.23)$$

where  $I$  is the identity operator, and  $b$  is not allowed to be trivially zero. Dividing through by  $e^{\lambda t}$ , it must be that

$$\lambda b = Lb = -(D + i\omega)b + \frac{K}{2} \int_{-\infty}^{\infty} b(\nu)g(\nu)d\nu. \quad (4.24)$$

Since the integral in Eq. (4.24) is just some constant, we can call it

$$A \equiv \frac{K}{2} \int_{-\infty}^{\infty} b(\nu)g(\nu)d\nu, \quad (4.25)$$

and then solve for  $b$  in Eq. (4.24):

$$b(\omega) = \frac{A}{\lambda + D + i\omega}. \quad (4.26)$$

We then use a self-consistency argument by substituting this into Eq. (4.25) for  $b$ :

$$A = \frac{K}{2} \int_{-\infty}^{\infty} \frac{Ag(\nu)}{\lambda + D + i\nu} d\nu. \quad (4.27)$$

We do not consider the  $A = 0$  solution because this would give us  $c(t, \omega) \equiv 0$ , which is not a valid eigenfunction. Then we are left with

$$1 = \frac{K}{2} \int_{-\infty}^{\infty} \frac{g(\nu)}{\lambda + D + i\nu} d\nu \quad (4.28)$$

as the equation for the eigenvalues  $\lambda$ .

We can further simplify this by using the following fact: if we assume that  $g(\omega)$  is even and that it never increases on  $[0, \infty)$ , which is true for most of the distributions that we are looking at, then there is at most one solution for  $\lambda$ , and if a solution exists, it is real [9]. This means we can multiply and divide the integrand

---

<sup>2</sup>This is completely equivalent to finding solutions of Eq. (4.19) of the separated form (4.21).

in Eq. (4.28) by the complex conjugate of the denominator to get

$$1 = \frac{K}{2} \int_{-\infty}^{\infty} \frac{\lambda + D - i\nu}{(\lambda + D)^2 + \nu^2} g(\nu) d\nu, \quad (4.29)$$

and the imaginary part will integrate to zero because it is an odd function of  $\nu$ , so

$$1 = \frac{K}{2} \int_{-\infty}^{\infty} \frac{\lambda + D}{(\lambda + D)^2 + \nu^2} g(\nu) d\nu. \quad (4.30)$$

This equation shows how the eigenvalue  $\lambda$  depends on  $K$ ,  $D$ , and  $g(\omega)$ .

### 4.3.2 Finding $K_C$ with Noise

The eigenvalue  $\lambda$  will tell us the stability of  $c$  [note Eq. (4.21)], and therefore the stability of  $r$ . If  $\lambda > 0$ , then  $c$  grows exponentially in time, and from Eq. (4.14) we see that  $r$  also grows exponentially, meaning the incoherent state is unstable. If  $\lambda < 0$ ,  $c$  decays, and  $r$  shrinks back down to zero, meaning the incoherent state is stable.

Notice that any eigenvalue  $\lambda$  must satisfy  $\lambda > -D$  so that the right side of Eq. (4.30) can be positive. This presents an interesting fact: with no noise,  $D = 0$ , which means that  $\lambda$  cannot be negative, and from the above discussion we know that  $\lambda$  must be negative for the incoherent state to be stable. The surprising result, then, is that the incoherent state cannot be linearly stable (only neutrally stable, with  $\lambda = 0$ ) without the presence of noise.

But as long as  $D > 0$ , the fundamental mode of  $\eta$  can be stable, and we find the critical crossover point to instability of the incoherent state by setting  $\lambda = 0$  in Eq. (4.30). This gives us the critical coupling  $K_C$  in the presence of noise:

$$K_C = 2 \left[ \int_{-\infty}^{\infty} \frac{D}{D^2 + \nu^2} g(\nu) d\nu \right]^{-1}. \quad (4.31)$$

### 4.3.3 Solving Explicitly for the Eigenvalue

We now have an equation [Eq. (4.30)] for finding the eigenvalue of  $c$ , the fundamental mode of the perturbation  $\eta$ . For some special cases of the distribution of natural frequencies  $g(\omega)$ , this eigenvalue can be found explicitly by carrying out the integration in Eq. (4.30).

For instance, in the case that all the oscillators are identical,  $g(\omega) = \delta(\omega)$ , so

$$1 = \frac{K}{2} \int_{-\infty}^{\infty} \frac{\lambda + D}{(\lambda + D)^2 + \nu^2} \delta(\nu) d\nu = \frac{K}{2} \frac{\lambda + D}{(\lambda + D)^2} = \frac{K}{2(\lambda + D)}, \quad (4.32)$$

implying that

$$\lambda = \frac{K}{2} - D. \quad (4.33)$$

We find  $K_C$  by setting  $\lambda = 0$ , so in this case

$$K_C = 2D. \quad (4.34)$$

For a uniform distribution over some interval of frequencies, the distribution function is given by  $g(\omega) = \frac{1}{2\gamma}$  when  $-\gamma \leq \omega \leq \gamma$  and  $g(\omega) = 0$  elsewhere. Performing the integration in Eq. (4.30) produces the eigenvalue

$$\lambda = \gamma \cot \frac{2\gamma}{K} - D, \quad (4.35)$$

and by setting  $\lambda = 0$  we see that

$$K_C = \frac{2\gamma}{\arctan \frac{\gamma}{D}}. \quad (4.36)$$

Finally, a Lorentzian distribution, given by

$$g(\omega) = \frac{\gamma}{\pi(\gamma^2 + \omega^2)}, \quad (4.37)$$

produces the eigenvalue

$$\lambda = \frac{K}{2} - D - \gamma, \quad (4.38)$$

and therefore has a critical coupling

$$K_C = 2(D + \gamma) = \beta^2 + 2\gamma.^3 \quad (4.39)$$

#### 4.3.4 The Continuous Spectrum

It turns out that the evolution equation for the first harmonic  $c$  of the perturbation [Eq. (4.19)] has both a discrete and a continuous spectrum. We have already found the discrete spectrum by solving Eq. (4.23) for  $\lambda$ . Here we finish the spectral analysis by finding the continuous spectrum.

The continuous spectrum of our linear operator  $L$  [Eq. (4.22)] is defined as the set of  $\lambda$  values that solve the eigenvalue equation

$$(L - \lambda I)b(\omega) = f(\omega), \quad (4.40)$$

---

<sup>3</sup> $\beta^2$  is simply an alternative parameter to  $D$  that specifies the amount of noise present in the system. We used  $\beta^2$  in our numerical simulations.

where  $f(\omega)$  is an arbitrary function of  $\omega$ . Analogously to the discrete eigenvalue problem, to find the continuous spectrum, we want  $L - \lambda I$  to be non-invertible, so that we *cannot* trivially solve for  $b(\omega)$  for an arbitrary  $f(\omega)$ . Therefore we seek  $\lambda$  that leave us unable to solve for  $b(\omega)$ . Using Eq. (4.22), Eq. (4.40) is equivalent to

$$-(\lambda + D + i\omega)b + \frac{K}{2} \int_{-\infty}^{\infty} b(\nu)g(\nu)d\nu = f(\omega). \quad (4.41)$$

As before when solving for the discrete spectrum, the integral term is just some constant, so we can call it  $A$ :

$$A \equiv \frac{K}{2} \int_{-\infty}^{\infty} b(\nu)g(\nu)d\nu. \quad (4.42)$$

We therefore see that if  $\lambda + D + i\omega = 0$ , Eq. (4.41) is not solvable in general; it would only be solvable in the special case that  $f(\omega) \equiv A$ . Thus the eigenvalues given by this method are the continuous set

$$\lambda = -D - i\omega, \quad (4.43)$$

where  $\omega$  ranges over all values where  $g(\omega) \neq 0$ .

We can furthermore show that this is the entire continuous spectrum. Suppose that there is an eigenvalue  $\lambda$  that is not in the discrete spectrum and does not satisfy Eq. (4.43). Then, solving Eq. (4.41) for  $b$ :

$$b(\omega) = \frac{A - f(\omega)}{\lambda + D + i\omega}. \quad (4.44)$$

But remember that if we are able to solve for  $b$ , then  $\lambda$  is *not* in the continuous spectrum. So if we can always solve for  $b$  in this case, then we must have already found all of the continuous spectrum. One last item to check is that we can solve for the  $A$  that goes in Eq. (4.44). To do this, we use a self-consistency argument by substituting this expression for  $b$  into the definition of  $A$ :

$$A = \frac{K}{2} \int_{-\infty}^{\infty} \frac{A - f(\nu)}{\lambda + D + i\nu} g(\nu)d\nu, \quad (4.45)$$

which, solving for  $A$ , gives

$$A \left( 1 - \frac{K}{2} \int_{-\infty}^{\infty} \frac{g(\nu)}{\lambda + D + i\nu} d\nu \right) = -\frac{K}{2} \int_{-\infty}^{\infty} \frac{f(\nu)g(\nu)}{\lambda + D + i\nu} d\nu \quad (4.46)$$

Since  $\lambda$  is assumed *not* to be in the discrete spectrum, then it must not satisfy Eq. (4.28). This means that the coefficient of  $A$  is nonzero, and we can solve for  $A$ . Thus Eq. (4.43) produces the entire continuous spectrum.

Notice from Eq. (4.43) that, since the noise parameter  $D$  is never negative, the real part of any  $\lambda$  in the continuous spectrum is always negative (or zero). This means that solutions from  $\lambda$  in the continuous spectrum will never be unstable. Thus we were justified in ignoring the continuous spectrum when solving for  $K_C$ , since the transition to instability of the incoherent state happens when  $\text{Re}(\lambda)$  becomes positive.

## 4.4 Numerical Simulations with Noise

Continuing with the numerical work started in Section 2.3, simulations were done for the Kuramoto model with noise. The noise was included by simply adding a term  $\xi$  to the Kuramoto equations as in Eq. (3.16). The correct form of  $\xi$  to use for each timestep is a random value chosen from a normal (Gaussian) distribution of mean zero and width  $\beta^2/\Delta t$ , where  $\beta^2$  defines the strength of the noise and  $\Delta t$  is the size of the timesteps used in the simulation [10]. The simulations can then be run in the same way as the noise-free case, giving results as shown in Figure 4.2. The FORTRAN code used for this simulation is listed in Appendix C.

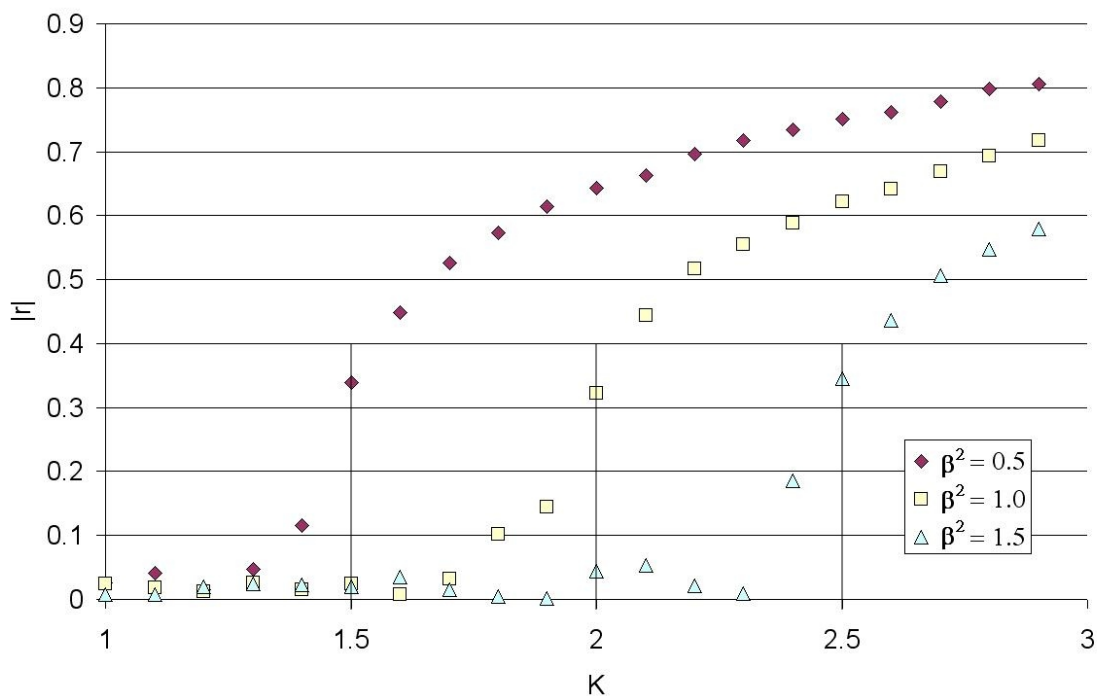


Figure 4.2: This plot shows how the magnitude of the order parameter  $|r|$  depends on the coupling  $K$  in the presence of noise.  $\beta^2$  sets the strength of the noise. These results are taken from the simulation of  $N = 5000$  oscillators with natural frequencies distributed according to a Lorentzian distribution with  $\gamma = 0.5$ , which was run on a network at the Ohio Supercomputer Center. From Eq. (4.39),  $K_C$  is predicted to occur at  $\beta^2 + 1$ . The expected values for  $K_C$  are shown as three vertical lines at 1.5, 2.0, and 2.5.

The numerical results for a Lorentzian distribution of natural frequencies agree with the analytical work [see Eq. (4.39)] in that the observed  $K_C$  appears to increase linearly with  $\beta^2$ . Also, although the observed values for  $K_C$  are lower than those expected from Eq. (4.39), this is believed to be a finite-size effect, which is seen in the case without noise as well (see Figure 2.3). Runs with smaller  $N$  not shown here were found to have a larger deviation from the expected  $K_C$ .

## 4.5 Evolution of Higher Harmonics

As we have seen, only the first harmonic  $c$  of the perturbation is important in regard to the phase synchronization of the Kuramoto model, since it is the only part of  $\eta$  that shows up in the expression for the order parameter  $r$ . Still, it is worth seeing what happens to the other harmonics  $\eta^\perp$ . This section follows section 4 in [11].

We have already found the evolution equation for  $\eta^\perp$  in Eq. (4.20). It is

$$\frac{\partial \eta^\perp}{\partial t} = D \frac{\partial^2 \eta^\perp}{\partial \theta^2} - \omega \frac{\partial \eta^\perp}{\partial \theta}. \quad (4.47)$$

We will write the solution  $\eta^\perp$  as a Fourier series in  $\theta$ . Remember that  $\eta^\perp$  has zero mean and no first harmonic by definition [see Eqs. (4.13) and (4.2)]. So the Fourier series is

$$\eta^\perp(\theta, t, \omega) = \sum_{|k| \geq 2}^{\infty} a_k(t, \omega) e^{ik\theta}. \quad (4.48)$$

Then, for each  $k$ , substitute into Eq. (4.47):

$$\frac{\partial a_k}{\partial t} e^{ik\theta} = -Dk^2 a_k e^{ik\theta} - ik\omega a_k e^{ik\theta} \quad (4.49)$$

$$\frac{\partial a_k}{\partial t} = (-Dk^2 - ik\omega) a_k, \quad (4.50)$$

which is solved to give

$$a_k(t, \omega) = a_k(0, \omega) e^{(-Dk^2 - ik\omega)t}. \quad (4.51)$$

Thus we have solved for the higher harmonics in terms of their initial conditions  $a_k(0, \omega)$ :

$$\eta^\perp(\theta, t, \omega) = \sum_{|k| \geq 2}^{\infty} a_k(0, \omega) e^{-k^2 D t} e^{ik(\theta - \omega t)}. \quad (4.52)$$

Notice first that  $\eta^\perp$  decays exponentially in time when  $D > 0$ . This means we have even more reason to ignore what is going on in the higher harmonics, since they will always damp out quickly if there is any noise in the system. Secondly, if  $D = 0$ ,  $\eta^\perp$  is an undamped rotating wave. In fact, when  $D = 0$ , it is true that any rotating wave  $f(\theta - \omega t, \omega)$  is a possible solution for  $\eta^\perp$ . This gives the interesting result that rotating waves of this form that involve only higher harmonics are neutrally stable to perturbations when there is zero noise.

## 4.6 Second Order Stability Analysis

In [11], Strogatz and Mirollo suggest a few problems that remain unfinished. One of these is carrying out the linear stability analysis to second order to see if a higher-order term will make affect stability. In this section we find that the stability of the incoherent state is in fact exactly the same when including second order terms.

### 4.6.1 Adding the Second Order Perturbation

The basic steps in the second order analysis are the same as with first order in Sections 4.1-4.3. First, we define the nature of the perturbation, this time with a second order term:

$$\rho(\theta, t, \omega) = \frac{1}{2\pi} + \epsilon\eta(\theta, t, \omega) + \epsilon^2\gamma(\theta, t, \omega), \quad (4.53)$$

and impose the same normalizability constraint on  $\gamma$ :

$$\int_0^{2\pi} \gamma(\theta, t, \omega) d\theta = 0. \quad (4.54)$$

Substituting Eq. (4.53) into the Fokker-Planck equation (3.19) gives

$$\epsilon \frac{\partial \eta}{\partial t} + \epsilon^2 \frac{\partial \gamma}{\partial t} = \epsilon D \frac{\partial^2 \eta}{\partial \theta^2} + \epsilon^2 D \frac{\partial^2 \gamma}{\partial \theta^2} - \frac{\partial}{\partial \theta} \left[ \left( \frac{1}{2\pi} + \epsilon\eta + \epsilon^2\gamma \right) v \right]. \quad (4.55)$$

Again, we are looking for  $v$ , so we first solve for  $r$ . By substituting Eq. (4.53) into Eq. (3.8), and recognizing that the constant  $1/2\pi$  again integrates to zero, we are left with



$$\begin{aligned}
re^{i\psi} &= \epsilon \int_0^{2\pi} \int_{-\infty}^{\infty} e^{i\theta} \eta(\theta, t, \omega) g(\omega) d\omega d\theta \\
&+ \epsilon^2 \int_0^{2\pi} \int_{-\infty}^{\infty} e^{i\theta} \gamma(\theta, t, \omega) g(\omega) d\omega d\theta.
\end{aligned} \tag{4.56}$$

Now define  $r_1$  as before, and also define  $r_2$ :

$$r_1 e^{i\psi} = \int_0^{2\pi} \int_{-\infty}^{\infty} e^{i\theta} \eta(\theta, t, \omega) g(\omega) d\omega d\theta \tag{4.57}$$

$$r_2 e^{i\psi} = \int_0^{2\pi} \int_{-\infty}^{\infty} e^{i\theta} \gamma(\theta, t, \omega) g(\omega) d\omega d\theta, \tag{4.58}$$

so that

$$r = \epsilon r_1 + \epsilon^2 r_2. \tag{4.59}$$

Then from the expression for  $v$  [Eq. (2.4)],

$$v = \omega + K(\epsilon r_1 + \epsilon^2 r_2) \sin(\psi - \theta) \tag{4.60}$$

$$\frac{\partial v}{\partial \theta} = -K(\epsilon r_1 + \epsilon^2 r_2) \cos(\psi - \theta). \tag{4.61}$$

This allows us to find the  $O(\epsilon^2)$  part of the final term in Eq. (4.55). Substituting Eqs. (4.60) and (4.61) and taking only terms up to  $O(\epsilon^2)$ , the final term becomes

$$\left[ \frac{K}{2\pi} (\epsilon r_1 + \epsilon^2 r_2) + K \epsilon^2 \eta r_1 \right] \cos(\psi - \theta) - \epsilon [\omega + \epsilon K r_1 \sin(\psi - \theta)] \frac{\partial \eta}{\partial \theta} - \epsilon^2 \omega \frac{\partial \gamma}{\partial \theta}. \tag{4.62}$$

Putting this back into Eq. (4.55) and doing some rearranging produces

$$\begin{aligned}
\epsilon \frac{\partial \eta}{\partial t} + \epsilon^2 \frac{\partial \gamma}{\partial t} &= \epsilon D \frac{\partial^2 \eta}{\partial \theta^2} - \epsilon \omega \frac{\partial \eta}{\partial \theta} + \epsilon \frac{K}{2\pi} r_1 \cos(\psi - \theta) \\
&+ \epsilon^2 D \frac{\partial^2 \gamma}{\partial \theta^2} + \epsilon^2 K \left[ \frac{r_2}{2\pi} + \eta r_1 \right] \cos(\psi - \theta) - \epsilon^2 K r_1 \sin(\psi - \theta) \frac{\partial \eta}{\partial \theta} - \epsilon^2 \omega \frac{\partial \gamma}{\partial \theta}.
\end{aligned} \tag{4.63}$$

The  $\epsilon$  terms are the same as those found in Eq. (4.12), so we can subtract them out. Then, dividing by  $\epsilon^2$ , we obtain the evolution equation for the second-order perturbation  $\gamma$ :

$$\frac{\partial \gamma}{\partial t} = D \frac{\partial^2 \gamma}{\partial \theta^2} + K \left[ \frac{r_2}{2\pi} + \eta r_1 \right] \cos(\psi - \theta) - K r_1 \sin(\psi - \theta) \frac{\partial \eta}{\partial \theta} - \omega \frac{\partial \gamma}{\partial \theta}. \tag{4.64}$$

## 4.6.2 Fourier Methods

To analyze the evolution of  $\gamma$ , we again use Fourier methods. As before,  $c(t, \omega)$  is defined to be the first harmonic of  $\eta$ . We now define  $s(t, \omega)$  to do the same for  $\gamma$ :

$$\gamma(\theta, t, \omega) = s(t, \omega)e^{i\theta} + s^*(t, \omega)e^{-i\theta} + \gamma^\perp(\theta, t, \omega). \quad (4.65)$$

By analogy with Eq. (4.14), we can write

$$r_1 e^{i\psi} = 2\pi \int_{-\infty}^{\infty} c^*(\omega, t)g(\omega)d\omega \quad (4.66)$$

$$r_2 e^{i\psi} = 2\pi \int_{-\infty}^{\infty} s^*(\omega, t)g(\omega)d\omega. \quad (4.67)$$

This tells us that  $r(t)$  depends only on the first harmonics  $c$  and  $s$  [see Eq. (4.59)].

With the same logic used to find Eq. (4.16), we can find the following parts of the evolution equation (4.64) in terms of  $c$  and  $s$ :

$$r_2 \cos(\psi - \theta) = \pi \left[ \left( \int_{-\infty}^{\infty} s^*(t, \omega)g(\omega)d\omega \right) e^{-i\theta} + \left( \int_{-\infty}^{\infty} s(t, \omega)g(\omega)d\omega \right) e^{i\theta} \right] \quad (4.68)$$

$$\eta r_1 \cos(\psi - \theta) = \eta\pi \left[ \left( \int_{-\infty}^{\infty} c^*(t, \omega)g(\omega)d\omega \right) e^{-i\theta} + \left( \int_{-\infty}^{\infty} c(t, \omega)g(\omega)d\omega \right) e^{i\theta} \right] \quad (4.69)$$

$$r_1 \sin(\psi - \theta) = -i\pi \left[ \left( \int_{-\infty}^{\infty} c^*(t, \omega)g(\omega)d\omega \right) e^{-i\theta} + \left( \int_{-\infty}^{\infty} c(t, \omega)g(\omega)d\omega \right) e^{i\theta} \right]. \quad (4.70)$$

After inserting these into Eq. (4.64), taking the derivatives, collecting terms, and simplifying, we get

$$\begin{aligned} & e^{i\theta} \left[ \frac{\partial s}{\partial t} + Ds + i\omega s - \frac{K}{2} \int_{-\infty}^{\infty} sg(\nu)d\nu - \pi K \left( \eta^\perp - i \frac{\partial \eta^\perp}{\partial \theta} \right) \int_{-\infty}^{\infty} cg(\nu)d\nu \right] \\ + & e^{-i\theta} \left[ \frac{\partial s^*}{\partial t} + Ds^* - i\omega s^* - \frac{K}{2} \int_{-\infty}^{\infty} s^*g(\nu)d\nu - \pi K \left( \eta^\perp + i \frac{\partial \eta^\perp}{\partial \theta} \right) \int_{-\infty}^{\infty} c^*g(\nu)d\nu \right] \\ + & \left[ \frac{\partial \gamma^\perp}{\partial t} - D \frac{\partial^2 \gamma^\perp}{\partial \theta^2} + \omega \frac{\partial \gamma^\perp}{\partial \theta} \right] \\ - & 2\pi K e^{2i\theta} \left[ c \int_{-\infty}^{\infty} cg(\nu)d\nu \right] - 2\pi K e^{-2i\theta} \left[ c^* \int_{-\infty}^{\infty} c^*g(\nu)d\nu \right] = 0. \end{aligned} \quad (4.71)$$

Since this must hold for all values of  $\theta$ , each bracketed item must equal zero. Specifically, notice that the  $e^{\pm 2i\theta}$  terms force either  $c^*(t, \omega) \equiv 0$  or [using Eq. (4.66)]

$$\int_{-\infty}^{\infty} c^*g(\nu)d\nu = r_1 e^{i\psi} \equiv 0. \quad (4.72)$$

Thus, by the definition of the order parameter (4.59), the first order perturbation  $\eta$  has no effect on  $r$  in the second order analysis. Furthermore, Eq. (4.72) forces every  $\eta^\perp$  term in Eq. (4.71) to vanish. Just as before, we are left with two equations:

$$\frac{\partial s}{\partial t} = -(D + i\omega)s - \frac{K}{2} \int_{-\infty}^{\infty} sg(\nu)d\nu \quad (4.73)$$

$$\frac{\partial \gamma^\perp}{\partial t} = D \frac{\partial^2 \gamma^\perp}{\partial \theta^2} - \omega \frac{\partial \gamma^\perp}{\partial \theta}. \quad (4.74)$$

Comparison with Eqs. (4.19) and (4.20) shows that these are exactly equivalent to the evolution equations for  $c$  and  $\eta^\perp$ . Thus analyzing the perturbation to second order gives the exact same behavior as doing a first order analysis.

# Conclusion

From rumbling generators to flashing fireflies, finding spontaneous synchronization in nature is both beautiful and mysterious. The Kuramoto model partially lifts the veil on this mystery, presenting a powerful way to study synchronization mathematically. With the few simplifications proposed by Kuramoto, we can predict the conditions under which phase and frequency synchronization will occur, and to what degree they will be present.

Noise can be an important factor in physical systems, yet is often neglected due to difficulties in merging it successfully with physical models. It is therefore impressive to find that random noise can be relatively easily dealt with in the Kuramoto model. Besides being able to solve explicitly for the effect of noise in many cases, it is interesting to find that synchronization happens in much the same way in noisy conditions as it does without noise.

Even in cases where the systems being studied break the limitations for finding explicit mathematical results with the model, numerical simulations have proven to be a useful alternative. My numerical results show that the simulations agree with the model's predictions, and they provide hints about the effects of including only a finite number of oscillators. Future work could use such simulations to study models similar to the Kuramoto model that are not as mathematically tractable.

Overall, the Kuramoto model provides a large mathematical realm to explore, with intriguing results around every corner. The fact that it connects with the prevalent natural phenomenon of synchronization establishes its distinction as a topic worthy of study to scientists of all kinds.

# Acknowledgments

I would like especially to thank Dr. Brad Trees, my advisor for this project, for his unwavering support and guidance in every area of this research. Thanks also goes to the rest of the Ohio Wesleyan Physics Department, who have all helped in their own way to see this paper to its final form. Finally, I gratefully acknowledge a grant of time from the Ohio Supercomputer Center, Grant #PQS0002-1.

# Appendix A

## The Vanishing Drift Integral

In solving for the steady solutions of the Kuramoto model, it is important that the drifting oscillators make no contribution to the order parameter. Using the fact that  $\rho(\theta + \pi, -\omega) = \rho(\theta, \omega)$  from Eq. (2.7) and our assumption that the distribution of natural frequencies is even [ $g(-\omega) = g(\omega)$ ], we can see why this is indeed the case.

Equation (2.11) gives the drifting oscillators' contribution to  $r$ :

$$\langle e^{i\theta} \rangle_{\text{drift}} = \int_{-\pi}^{\pi} \int_{|\omega| > Kr} e^{i\theta} \rho(\theta, \omega) g(\omega) d\omega d\theta \quad (\text{A.1})$$

$$= \int_{-\pi}^{\pi} \int_{-\infty}^{-Kr} e^{i\theta} \rho(\theta, \omega) g(\omega) d\omega d\theta + \int_{-\pi}^{\pi} \int_{Kr}^{\infty} e^{i\theta} \rho(\theta, \omega) g(\omega) d\omega d\theta. \quad (\text{A.2})$$

The left-hand integral in Eq. (A.2) can be rewritten as

$$- \int_{-\pi}^{\pi} \int_{\infty}^{Kr} e^{i\theta} \rho(\theta, -\omega) g(-\omega) d\omega d\theta. \quad (\text{A.3})$$

Now we change variables to  $\theta' = \theta - \pi$  and use the fact that  $g(-\omega) = g(\omega)$  to get

$$- \int_{-2\pi}^0 \int_{\infty}^{Kr} e^{i\theta'} e^{i\pi} \rho(\theta' + \pi, -\omega) g(\omega) d\omega d\theta'. \quad (\text{A.4})$$

Flipping the  $\omega$  interval and factoring out the  $e^{i\pi} = -1$  produces two negatives that cancel, and we know that  $\rho(\theta' + \pi, -\omega) = \rho(\theta', \omega)$ , so the integral becomes

$$- \int_{-2\pi}^0 \int_{Kr}^{\infty} e^{i\theta'} \rho(\theta', \omega) g(\omega) d\omega d\theta'. \quad (\text{A.5})$$

Due to the periodic boundary conditions, we can shift the  $\theta'$  interval without changing anything, leaving us with

$$- \int_{-\pi}^{\pi} \int_{K_r}^{\infty} e^{i\theta'} \rho(\theta', \omega) g(\omega) d\omega d\theta'. \quad (\text{A.6})$$

This is exactly the negative of the second integral in Eq. (A.2), so they cancel and

$$\langle e^{i\theta} \rangle_{\text{drift}} = 0. \quad (\text{A.7})$$

## Appendix B

# Deriving a Fokker-Planck Equation for the Kuramoto Model

To produce a Fokker-Planck equation<sup>1</sup>, first write the Kuramoto model equations (1.4) with noise in the form

$$d\theta_i = \left( \omega_i + \frac{K}{N} \sum_{j=1}^n \sin(\theta_j - \theta_i) \right) dt + \sqrt{\beta^2 dt} N(0, 1), \quad i = 1, \dots, N. \quad (\text{B.1})$$

To simplify the notation, define

$$v_i \equiv \omega_i + \frac{K}{N} \sum_{j=1}^n \sin(\theta_j - \theta_i), \quad (\text{B.2})$$

so that  $v_i$  is the instantaneous angular velocity of oscillator  $i$  in the absence of noise. Then Eq. (B.1) becomes

$$d\theta_i = v_i dt + \sqrt{\beta^2 dt} N(0, 1), \quad i = 1, \dots, N. \quad (\text{B.3})$$

We now make use of the identity<sup>2</sup>

$$\int f(\theta) \frac{\partial \rho}{\partial t} d\theta = \left\langle \frac{df(\theta)}{dt} \right\rangle. \quad (\text{B.4})$$

Expanding  $df$  to second order gives

$$df = \frac{\partial f}{\partial \theta} d\theta + \frac{\partial^2 f}{\partial \theta^2} \frac{(d\theta)^2}{2}, \quad (\text{B.5})$$

---

<sup>1</sup>This derivation follows the same general form as in Appendix B in [8].

<sup>2</sup>This comes from differentiating the identity  $\int f(\theta) \rho(\theta, \omega, t) d\theta = \langle f(\theta) \rangle$ , one form of the well-known ergodic hypothesis. This hypothesis states that the average value of some measurable quantity will be the same whether you take the average value of a large ensemble of systems at a single time or the average value of a single system over a long time.



which becomes the following when we substitute Eq. (B.3) and drop terms with factors of  $(dt)^2$  or smaller:

$$df = \frac{\partial f}{\partial \theta} \left( v dt + \sqrt{\beta^2 dt} N(0, 1) \right) + \frac{\partial^2 f}{\partial \theta^2} \frac{\beta^2 dt}{2} N^2(0, 1). \quad (\text{B.6})$$

We can now substitute into Eq. (B.4) and notice that  $\langle \sqrt{\beta^2 dt} N(0, 1) \rangle = \langle \sqrt{\beta^2 dt} \rangle \langle N(0, 1) \rangle = 0$  (since the mean of  $N(0, 1)$  is zero by definition) and  $\langle N^2(0, 1) \rangle = 1$  (since the average of the square is equal to the variance when the mean is zero) to get

$$\int f(\theta) \frac{\partial \rho}{\partial t} d\theta = \left\langle \frac{df}{d\theta} v + \frac{\beta^2}{2} \frac{d^2 f}{d\theta^2} \right\rangle. \quad (\text{B.7})$$

Now express the right-hand side of this equation as an integration over phase space:

$$\int f(\theta) \frac{\partial \rho}{\partial t} d\theta = \int \left( \frac{df}{d\theta} v + \frac{\beta^2}{2} \frac{d^2 f}{d\theta^2} \right) \rho d\theta. \quad (\text{B.8})$$

Integrate the right-hand side by parts, dropping the surface terms (since we have periodic boundaries) to obtain

$$\int f(\theta) \frac{\partial \rho}{\partial t} d\theta = \int f(\theta) \left( -\frac{\partial \rho}{\partial \theta} v + \frac{\beta^2}{2} \frac{\partial^2 \rho}{\partial \theta^2} \right) d\theta. \quad (\text{B.9})$$

For this equation to hold for an arbitrary function  $f$ , it must be that

$$\frac{\partial \rho}{\partial t} = \frac{\beta^2}{2} \frac{\partial^2 \rho}{\partial \theta^2} - \frac{\partial}{\partial \theta} (\rho v). \quad (\text{B.10})$$

This is the Fokker-Planck equation that is equivalent to the Kuramoto model. In Strogatz and Mirollo [11], this is written as

$$\frac{\partial \rho}{\partial t} = D \frac{\partial^2 \rho}{\partial \theta^2} - \frac{\partial}{\partial \theta} (\rho v), \quad (\text{B.11})$$

so

$$D = \frac{\beta^2}{2}. \quad (\text{B.12})$$

Both  $D$  and  $\beta^2$  are parameters that describe the amount of noise in the system.  $\beta$  has units of angular frequency, and  $D$  has units of angular frequency squared. We used  $\beta^2$  in our numerical simulations.

# Appendix C

## Example FORTRAN Code

```
! kuramoto_lorentzian_noise.f90
!  
! Bryan Daniels
! 9-25-2004
! 1-04-2005 added noise
! 2-09-2005 finalized noise
!  
! Numerical simulation of the Kuramoto model.
! N globally coupled oscillators.
! Gaussian noise term added each timestep.
!  
  
implicit none  
  
integer N  
parameter (N=5000) ! number of oscillators  
  
double precision, dimension(N):: Theta, dTheta_dtau, omega, Theta_out, eta  
double precision tau, Delta_tau, K, Delta_K, r, phi, gamma, pi, beta_squared, Delta_beta_squared  
integer timesteps, i, j, t, num_K, l  
  
K = 1.0d0      ! initial coupling  
Delta_K = 0.2d0 ! K step size  
Delta_tau = .01d0 ! time step size  
timesteps = 5e5 ! number of time steps until we calculate r  
num_K = 10     ! number of K values to test  
gamma = 0.5d0  ! defines the width of the distribution g(omega)  
beta_squared = 0.5d0 ! strength of noise  
Delta_beta_squared = 0.5d0  
pi = 4.d0*datan(1.d0)  
  
open(unit=40, file='lorentzian_1000_gamma=0.5_beta_squared=varying.txt', status='unknown')  
open(unit=50, file='Omega_1000_gamma=0.5_beta_squared=varying.txt', status='unknown')
```

```

open(unit=60, file='psi_1000_gamma=0.5_beta_squared=varying.txt', status='unknown')
open(unit=70, file='r_1000_gamma=0.5_beta_squared=varying.txt', status='unknown')

! set natural frequencies to lorentzian distribution
call lorentzian(gamma, N, omega)

close(40)

! loop over beta_squared values
do 950 l = 1,4

    write(70,*) "Beta^2 = ", beta_squared

! loop over K values
do 900 i = 1,num_K

    write(50,*) "K = ", K
    write(50,*) "Beta^2 = ", beta_squared
    write(60,*) "K = ", K
    write(60,*) "Beta^2 = ", beta_squared

    tau = 0.0d0

    ! initialize phases randomly
    call random_seed
    do 111 t=1,N
call random_number(Theta(t))
Theta(t) = Theta(t) * 2.d0*pi
111 continue

    do 800 t = 1,timesteps

        call random_array(eta,N,beta_squared/Delta_tau)
        call derivs(tau, Theta, dTheta_dtau, N, K, eta, omega)
        call rk4(Theta, dTheta_dtau, N, tau, Delta_tau, Theta_out, K, beta_squared, eta, omega)
        Theta = Theta_out

        tau = tau + Delta_tau

800    continue

call find_order_param(Theta, r, phi, N)
write(*,*) K, r
write(70,*) K, r

do 500 j = 1,N
    write(50,*) omega(j), "    ", dTheta_dtau(j)
    write(60,*) omega(j), "    ", MOD(Theta(j),2*pi)

```

```

500 continue

      K = K + Delta_K

900 continue

      K = 1.0d0
      beta_squared = beta_squared + Delta_beta_squared

950 continue

stop
end

! lorentzian
!
! produces an array of random values for the natural frequencies omega(i)
! uses lorentzian distribution (rejection method); produces values
! from -10*gamma to 10*gamma
! takes a value for gamma (defines width), and N, the size of the array
! returns the array gamma with random values

subroutine lorentzian(gamma, N, omega)

implicit none
      integer N
double precision, dimension(N)::i_thermal, omega
double precision pi, gamma, random1, random2, p, p_max
integer d
call random_seed

pi = 4.d0*datan(1.d0)

p_max = 1/(pi*gamma)

do 75 d=1,N

50 call random_number(random1)
random1 = random1*20.d0*gamma - 10.d0*gamma
p = gamma / (pi * (gamma*gamma + random1*random1))
call random_number(random2)
random2 = random2*p_max
if (random2 > p) go to 50
omega(d) = random1

75 continue

return

```

```

end

! rk4
!
! rk4 uses the fourth-order runge-kutta method to advance the
!   solution over an interval h
! returns the advanced value yout
! uses subroutine derivs to obtain values for the derivatives
! (from Numerical Recipies)
! **with noise**
subroutine rk4(y,dydx,n,x,h,yout,K,beta_squared,eta,omega)

implicit none
    integer n
double precision, dimension(n) :: y, dydx, yout, yt, dyt, dym, omega, eta
double precision h, hh, h6, x, xh, K, beta_squared
integer i
external derivs

hh=h*0.5
h6=h/6.d0
xh=x+hh
do 11 i=1,n
yt(i)=y(i)+hh*dydx(i)
11 continue

    call derivs(xh,yt,dyt,n,K,eta,omega)
do 12 i=1,n
yt(i)=y(i)+hh*dyt(i)
12 continue

    ! use same noise array as last
call derivs(xh,yt,dym,n,K,eta,omega)
do 13 i=1,n
yt(i)=y(i)+h*dym(i)
dym(i)=dyt(i)+dym(i)
13 continue

    call derivs(x+h,yt,dyt,n,K,eta,omega)
do 14 i=1,n
yout(i)=y(i)+h6*(dydx(i)+dyt(i)+2.d0*dym(i))
14 continue

return
end

! derivs
!
```

```

! calculates the time derivative of Theta using the Kuramoto model
! **with noise**
! (using equation 1-3 in notes plus noise)
! returns the array dTheta_dtau
subroutine derivs(tau, Theta, dTheta_dtau, N, K, eta, omega)

    implicit none
    integer N
    double precision, dimension(N)::Theta, dTheta_dtau, omega, eta
    double precision tau, K, r, phi
    integer i

    call find_order_param(Theta, r, phi, N)

    do 100 i=1,N

        dTheta_dtau(i) = omega(i) + K*r*d sin(phi-Theta(i)) + eta(i)

100    continue

    return
end

! find_order_param
!
! computes the complex order parameter,
! returned as the variables r and phi,
! where r is the magnitude and phi is the angle
subroutine find_order_param(theta, r, phi, N)

    implicit none
        integer N
    double precision, dimension(N)::theta
    double precision r, phi, real_sum, imag_sum
    integer j

    real_sum = 0.d0
    imag_sum = 0.d0

    do 200 j=1,N
        real_sum = real_sum + dcos(theta(j))
        imag_sum = imag_sum + dsin(theta(j))
    200    continue
    real_sum = real_sum/N
    imag_sum = imag_sum/N

    r = dsqrt((real_sum)**2 + (imag_sum)**2)
        phi = dacos(real_sum/r)

```

```

    return
end

! random_array(x)
!
! returns an array of N random numbers
! gaussian distribution, mean zero, width specified as parameter

subroutine random_array(array, N, width)

    implicit none
    double precision, dimension(N):: array
    double precision width
    integer N, i

    do 300 i=1,N
        call normal_random_num(array(i))
        array(i) = dsqrt(width) * array(i)
300    continue

    return
end

! normal_random_num(x)
!
! returns a random value from a gaussian probability distribution
! with mean 0 and width 1.
! uses gaussian distribution (rejection method); produces values
! from -10 to 10

subroutine normal_random_num(x)

    implicit none
    double precision x, pi, p, p_max, random1, random2

    pi = 4.d0*datan(1.d0)
    p_max = 1/sqrt(2*pi)

    50 call random_number(random1)
    random1 = random1*20.d0 - 10.d0
    p = exp(-(random1*random1)/2) / sqrt(2*pi)
    call random_number(random2)
    random2 = random2*p_max
    if (random2 > p) go to 50
    x = random1
    return
end

```

# References

- [1] Pikovsky, Rosenblum, and Kurths, *Synchronization* (Cambridge University Press, Cambridge, 2001).
- [2] S. H. Strogatz, *Sync* (Hyperion, New York, 2003).
- [3] S. H. Strogatz, *Nonlinear Dynamics and Chaos* (Addison-Wesley, Reading, MA, 1994).
- [4] S. H. Strogatz, *Physica D* **143**, 1 (2000).
- [5] Y. Kuramoto, *Chemical Oscillations, Waves, and Turbulence* (Springer-Verlag, New York, 1984).
- [6] Kiss, Zhai, Hudson, *Science* **296**, 1676 (2002).
- [7] B. C. Daniels, S. T. M. Dissanayake, and B. R. Trees, *Phys. Rev. E* **67**, 026216 (2003).
- [8] Don S. Lemons, *An Introduction to Stochastic Processes in Physics* (Johns Hopkins University Press, Baltimore, Maryland, 2002).
- [9] R. E. Mirollo and S. H. Strogatz, *J. Stat. Phys.* **60**, 245 (1990).
- [10] C. D. Tesche and J. Clarke, *J. Low Temp. Phys.* **29**, 301 (1977).
- [11] Steven H. Strogatz and Renato E. Mirollo, *J. Stat. Phys.* **63**, 613 (1991).